



**A novel HMGB1 neutralizing chimeric antibody attenuates
DILI and post-injury inflammation**

Journal:	<i>Hepatology</i>
Manuscript ID	HEP-15-2165.R1
Wiley - Manuscript type:	Original
Date Submitted by the Author:	04-Mar-2016
Complete List of Authors:	<p>Lundbäck, Peter; Karolinska Institutet, Medicine, Solna Lea, Jonathan; University of Liverpool, Molecular and Clinical Pharmacology Sowinska, Agnieszka; Karolinska Institutet, Medicine, Solna Ottosson, Lars; Karolinska Institutet, Women's and Children's Health, Solna Melin Fürst, Camilla; Lund University, Translational Medicine Steen, Johanna; Karolinska Institutet, Medicine, Solna Aulin, Cecilia; Karolinska Institutet, Medicine, Solna Clarke, Joanna; University of Liverpool, Molecular and Clinical Pharmacology Kipar, Anja; University of Liverpool, Molecular and Clinical Pharmacology Klevenvall, Lena; Karolinska Institutet, Women's and Children's Health, Solna Yang, Huan; The Feinstein Institute for Medical Research, Biomedical Science Palmblad, Karin; Karolinska Institutet, Women's and Children's Health, Solna Park, B. Kevin; University of Liverpool, Translational Medicine Tracey, Kevin; The Feinstein Institute for Medical Research, Biomedical Science Blom, Anna; Lund University, Translational Medicine Andersson, Ulf; Karolinska Institutet, Women's and Children's Health, Solna Antoine, Daniel; University of Liverpool, Molecular and Clinical Pharmacology Erlandsson Harris, Helena; Karolinska Institutet, Medicine, Solna</p>
Keywords:	Inflammation, therapeutics, acetaminophen, liver injury, alarmins

Title: A novel HMGB1 neutralizing chimeric antibody attenuates DILI and post-injury inflammation

Running head: A novel therapeutic antibody targeting HMGB1

Peter Lundbäck¹, Jonathan D. Lea², Agnieszka Sowinska¹, Lars Ottosson³, Camilla Melin Fürst⁴, Johanna Steen¹, Cecilia Aulin¹, Joanna I. Clarke², Anja Kipar², Lena Klevenvall³, Huan Yang⁵, Karin Palmblad³, B. Kevin Park², Kevin J. Tracey⁵, Anna M. Blom⁴, Ulf Andersson³, Daniel J. Antoine^{2,#}, and Helena Erlandsson Harris^{1,#}

¹Department of Medicine, Rheumatology Unit, Karolinska Institutet, Stockholm, Sweden;

²MRC Centre for Drug Safety Science, Department of Molecular & Clinical Pharmacology, Liverpool University, Liverpool, UK;

³Department of Women's and Children's Health, Karolinska Institutet, Stockholm, Sweden;

⁴Section of Medical Protein Chemistry, Department of Translational Medicine, Lund University, Malmö, Sweden;

⁵Laboratory of Biomedical Science, The Feinstein Institute for Medical Research, Manhasset, USA

[#]D.J.A and H.EH. shared last authorship

Corresponding author:

1. Peter Lundbäck, Rheumatology research laboratory, CMM L8:04, Dept Medicine, Karolinska Institutet, Karolinska University Hospital, SE-17176, Stockholm, Sweden, telephone: +46-735321201, email: peter.lundback@ki.se
2. Helena Erlandsson Harris, Rheumatology research laboratory, CMM L8:04, Dept Medicine, Karolinska Institutet, Karolinska University Hospital, SE-17176, Stockholm, Sweden, telephone: +46-735321201, email: helena.harris@ki.se
3. Daniel J. Antoine, MRC Centre for Drug Safety Science, Department of Molecular & Clinical Pharmacology, Liverpool University, Liverpool, UK, email: D.Antoine@liverpool.ac.uk

Word count: 6524 (incl. references 1332)

Figures main manuscript = 7

List of Abbreviations: Drug-induced liver injury (DILI), Acetaminophen (APAP), Acute liver injury (ALI), Acetaminophen-induced acute liver injury (APAP-ALI), Acute liver failure (ALF), N-acetylcysteine (NAC), High mobility group box 1 (HMGB1), Ischemia-reperfusion (I/R), Alcoholic liver disease (ALD), alanine aminotransferase (ALT), Monoclonal antibody (mAb), Surface plasmon resonance (SPR), Intraperitoneal (IP), Cytometric bead array (CBA), Endoglycosidase-S (endoS), Normal human serum (NHS), Fcγ receptors (FcγR), *Lens culinaris* agglutinin (LCA), Aggregated human IgG (Agg.IgG),

Financial Support

This study was supported by the Swedish Medical research council (No 2012-1870), The Swedish Cancer Foundation and Karolinska Institutet.

Abstract

Acetaminophen (APAP) overdoses are of major clinical concern. Growing evidence underlines a pathogenic contribution of sterile post-injury inflammation in APAP-induced acute liver injury (APAP-ALI) and justifies development of anti-inflammatory therapies with therapeutic efficacy beyond the therapeutic window of the only current treatment option, N-acetylcysteine (NAC).The inflammatory mediator high mobility group box 1 (HMGB1) is a key regulator of a range of liver injury conditions and is elevated in clinical and preclinical APAP-ALI. The anti-HMGB1 antibody (m2G7) is therapeutically beneficial in multiple inflammatory conditions and anti-HMGB1 polyclonal antibody treatment improves survival in a model of APAP-ALI. Herein, we developed and investigated the therapeutic efficacy of a partly humanized anti-HMGB1 monoclonal antibody (h2G7) and identified its mechanism of action in preclinical APAP-ALI. The mouse anti-HMGB1 monoclonal antibody (m2G7) was partly humanized (h2G7) by merging variable domains of m2G7 with human antibody-Fc backbones. Effector function deficient variants of h2G7 were assessed in comparison with h2G7 *in vitro* and in preclinical APAP-ALI. h2G7 retained identical antigen-specificity and comparable affinity as m2G7. 2G7 treatments significantly attenuated APAP-induced serum elevations of ALT, miR-122 and completely abrogated markers of APAP-induced inflammation (TNF, MCP-1 and CXCL-1) with prolonged therapeutic efficacy as compared to NAC. Removal of complement and/or Fc receptor binding did not affect h2G7 efficacy.

Conclusion: This is the first report describing the generation of a partly humanized HMGB1-neutralizing antibody with validated therapeutic efficacy and importantly, with a prolonged therapeutic window as compared to NAC in APAP-ALI. The therapeutic effect was mediated via HMGB1 neutralization and attenuation of post-injury inflammation. These results represent important progress towards clinical implementation of HMGB1-specific therapy as a means to treat APAP-ALI and other inflammatory conditions.

Introduction

Drug-induced liver injury (DILI) is the leading cause of acute liver injury (ALI), which is both a clinical concern and results in drug attrition, issuing of black box warnings and drug withdrawal from the market (1). Acetaminophen (APAP) is an analgesic and antipyretic and is generally safe when taken at therapeutic dose, however intentional or unintentional overdoses can lead to APAP-induced acute liver injury (APAP-ALI) and represent around 50% of all cases of acute liver failure (ALF) (2, 3). Clinical APAP intoxication is counteracted by peroral or intravenous administration of N-acetylcysteine (NAC), which has a narrow window for therapeutic intervention. Untreated, APAP overdoses can lead to fulminant liver failure and the clinical outcome ranges from full recovery, a need of liver transplantation or even death. The post APAP associated inflammation (especially innate immune activation), resulting from a substantial hepatocellular necrosis, is negatively associated with poor clinical outcome (i.e. need for liver transplant or death). For late presenting patients, in whom inflammatory responses are fulminant (4), there are no effective treatment options for severe cases of ALF beside liver transplantation. Due to the shortage of potential liver donors and cost of liver transplantations, there is an urgent need for development of alternative therapeutic strategies with broader therapeutic time windows than NAC, including immunomodulatory drugs, in preventing APAP-ALI progression.

High mobility group box 1 (HMGB1) was discovered 16 years ago as an endogenous inflammatory mediator and now serves as a prototype for the class of pro-inflammatory mediators denoted Alarmins. Alarmins are released passively during cell death or from stressed cells. During infectious and sterile inflammatory conditions, HMGB1 is also actively released by immune cells, enhancing and perpetuating inflammation and thus contribute to the pathogenesis of a great number of inflammatory diseases. The diverse inflammatory functions of HMGB1 are mediated via multiple, different reciprocal receptors. Global structural

changes associated with cysteine redox modifications of HMGB1 control its receptor usage and thereby its bioactivities. HMGB1 induces cell migration in its fully reduced, all-thiol form when interacting with CXCL-12 and CXCR-4 (5) whereas cytokine production is induced by the disulfide form interacting with the MD-2/TLR4 receptor complex (6, 7). Furthermore, HMGB1 has also been demonstrated to signal via RAGE, TLR2, TLR9, CD24/Siglec, and TIM-3 (8), with undetermined requirements for possible post-translational modifications. Additionally, the active secretion of HMGB1 is regulated by acetylation of HMGB1 (9), an HMGB1-specific modification that negatively correlates with APAP-ALI patient outcome (10).

HMGB1 plays a critical role in a wide array of liver disease conditions, including liver ischemia-reperfusion (I/R) injury, alcoholic liver disease (ALD), cholestasis and DILI. In liver I/R injury, necrotic cell death is prominent and HMGB1 is released (11). The pathogenic contribution of HMGB1 in hepatic I/R has recently been shown through blockade of the interaction between HMGB1 and MD-2 (7). Acetylated HMGB1 has been recorded in ALD patients and ethanol-fed mice, demonstrating an inflammatory component and active HMGB1 release in ALD. Furthermore, conditional hepatocyte ablation of *Hmgb1* is protective in a mouse model of ethanol-induced liver injury (12). Similar HMGB1 isoforms have been recorded in obstructive cholestasis patients (13), supporting an active release and inflammatory role of HMGB1 in this disease as well. HMGB1 is required for the post-APAP injury inflammation and has been shown to be pivotal in the progression of APAP-ALI and hepatocyte-specific HMGB1 deficiency improves survival (14). In a clinical setting, HMGB1 serves as a promising sensitive and specific biomarker of APAP-ALI, outperforming alanine aminotransferase (ALT) as marker of progression and as indicator of outcome (2, 10). The initial APAP-induced hepatocyte necrosis results in an initial release of all-thiol HMGB1. This leads to recruitment and activation of immune cells, which propagate the inflammatory

response, resulting in increased hepatocyte death and exacerbation of injury (14). HMGB1-specific antibody treatments have consolidated the pathogenic contribution of HMGB1 in APAP-ALI, demonstrating increased survival (15).

Therapies targeting either the release of HMGB1, interfering with HMGB1-receptor signaling or directly antagonizing HMGB1 (i.e. box A therapy) ameliorate disease severity and promote survival in a wide spectrum of experimental disease models (16). These therapies are however unspecific in the sense that they may affect other ligand-receptor interactions or signaling pathways utilized by other molecules than HMGB1. They may thus not be suitable for clinical use. Importantly, targeting HMGB1 with the use of antibodies specifically affects extracellular HMGB1 bioactivities but will not interfere with its intracellular functions. Successful HMGB1-specific polyclonal antibody therapy was first described in an acute inflammatory model of sepsis (17) and later in a chronic setting of experimental arthritis models (18). Polyclonal and monoclonal antibody (mAb)-based therapies are powerful tools in preclinical research. However, long-term clinical success in humans with such antibodies is hampered by the inherent immunogenicity of xenogeneic antibodies that may cause safety issues and a negative impact on the clinical efficacy (19). The development of humanized antibodies has significantly reduced the restricting xenogeneic immune responses. Chimeric antibodies, humanized antibodies with the antigen-binding region kept xenogenic, targeting self-antigens are presently used successfully to treat cancer (anti-CD20/rituximab), graft-versus-host disease (anti-CD25/basiliximab) and various autoimmune diseases (anti-TNF/infliximab). The heterogeneity of diseases or disorders with an inflammatory component emphasizes a continuous search for treatment refinement and creation of future therapies that specifically targets novel pathogenic molecules.

To enable development of HMGB1-targeted therapy for clinical use, we set out to engineer a chimeric anti-HMGB1 mAb (h2G7) by preserving the variable regions of an

extensively studied and effective mouse mAb (m2G7) with recorded beneficial anti-inflammatory effects in multiple preclinical models (Supplementary Table 1). To verify well-maintained beneficial therapeutic effects we utilized a highly HMGB1-dependent experimental model of APAP-ALI, which established that h2G7 provided equal therapeutic benefit as its murine analog. By modification of the CH2 domain we could generate a variant of h2G7 unable to activate the classical complement pathway (K322A mutant), and an h2G7 variant incapable of binding Fc-receptors (endoS-treated h2G7). By comparing the therapeutic *in vivo* efficacy of these three mAb variants we conclude that h2G7 treatment alleviated APAP-ALI via HMGB1 neutralization and has a prolonged therapeutic window as compared to NAC treatment.

Materials and methods

A detailed description of experiments is described in supplementary methods.

A chimeric anti-HMGB1 antibody (h2G7) with human IgG1 isotype was generated as described previously (20, 21). Briefly, DNA encoding the 2G7 mouse variable immunoglobulin domains was PCR amplified (Supplementary Table_2) and subcloned into plasmids encoding human constant domains. Antibody specificity was tested by coating plates with HMGB1, box A or box B followed by titration with increasing concentrations of mAbs. Affinities were analyzed by SPR. Briefly, mAbs were immobilized on a CM5-dextran chip and recombinant HMGB1 was injected at various concentrations (0nM, 55nM, 110nM, 220nM and 880nM). Determination of dissociation constants was performed using Langmuir-binding.

Male C57BL/6J or CD-1 mice (Charles River) were fasted (15-16h) before intraperitoneal (IP) injection of APAP (530 or 300mg/kg when indicated)(Supplementary Fig.

1
2
3 1). At 2h post-APAP (or 6h when indicated), 300µg of anti-HMGB1 antibodies, box A, E2
4 (irrelevant isotype control) or 500mg/kg NAC were injected IP. At 10h post-APAP (or 24h
5 when indicated), liver injury was determined by histology, serum ALT and expression of
6
7 miR-122. Inflammatory mediators were analyzed by cytometric bead array (CBA)(BD
8 Bioscience).

9
10
11
12
13
14
15 Effector function deficient variants of h2G7, incapable of binding complement or Fc
16 receptors were generated by site-directed mutagenesis (K322A, Supplementary Table_2) or by
17 endoglycosidase-S (endoS) treatment. Inability to activate complement was validated by a
18 decrease in C1q deposition from normal human serum (NHS). Antibody deglycosylation was
19 validated by a characteristic mass-shift (SDS-PAGE analysis) and LCA binding. Briefly,
20 antibodies were coated onto plates followed by addition of biotinylated-LCA and
21 subsequently visualized with Streptavidin-HRP and TMB. FcγR-binding was performed by
22 binding of antibodies to human CD64 coated plates or to live THP-1 cells. For binding to
23 THP-1 cells, h2G7 variant antibodies were incubated with cells followed by detection with a
24 FITC-conjugated F(ab')₂ anti-human antibody.
25
26
27
28
29
30
31
32
33
34
35
36

37
38 Statistical analysis for *in vivo* studies was performed with Kruskal-Wallis (Dunns post-
39 test) and for *in vitro* data, one-way ANOVA was performed where indicated. All statistical
40 analysis was performed using Graphpad Prism.
41
42
43
44
45
46
47
48
49
50
51
52
53
54
55
56
57
58
59
60

Results

Characterization of chimeric 2G7 mAb bioactivities

We merged the variable domains of 2G7, obtained from mouse (m2G7) hybridoma cells, with plasmids encoding the human IgG γ 1 isotype and IgG κ backbone in order to generate a chimeric anti-HMGB1 antibody (h2G7) (Fig. 1A). The specific parent anti-HMGB1 antibody (m2G7), that does not recognize HMGB2, binds to the amino acids 53-63 within the box A domain of rodent and human HMGB1 (22). Since antibody specificity may be influenced by a change of IgG isotype (23), we examined the antigen-specificity of h2G7 compared to m2G7. In similarity to m2G7, h2G7 displayed dose-dependent binding to full-length HMGB1 and the box A domain but not to the box B domain (Fig. 1B). By utilizing surface plasmon resonance (SPR) we defined the antibody binding affinities for m2G7 (K_d 170nM) and h2G7 (K_d 130nM) (Fig. 1C). This suggests that h2G7 had a slightly higher affinity towards HMGB1 as compared to its murine counterpart, although the recorded affinities were within the same order of magnitude. The human irrelevant IgG1 isotype control (E2) (20) did not bind to HMGB1, or the box A or box B domains (Fig. 1B and C). Distinct functional HMGB1 cysteine redox isoforms are present during different phases of APAP-induced inflammation (6, 15) and it was previously unknown whether 2G7 selectively binds to any of these redox isoforms. We therefore evaluated the binding capacity of m2G7 (Fig. 1D) and h2G7 (Fig. 1E) to all-thiol, disulfide and sulphonyl HMGB1. Both m2G7 and h2G7 displayed equal binding to all three isoforms tested indicating that 2G7 has the capacity to antagonize HMGB1 during separate stages of inflammation.

Equivalent therapeutic effects of h2G7 and m2G7

The therapeutic *in vivo* effects of h2G7 were evaluated in an experimental model of APAP-induced ALI (Supplementary Fig. 1). The pathogenic importance of HMGB1 in this model has previously been established by several reports (2, 7, 15, 24, 25). Non-APAP challenged C57BL/6 mice were treated with PBS (vehicle), h2G7, m2G7 or the control E2 antibody. None of the treatments significantly affected hepatic glutathione (GSH) levels as compared to the PBS control, indicating that the treatments alone did not affect the hepatic APAP-scavenging ability or APAP-bioconversion (Fig. 2A). No difference was recorded between the treatment groups in non-APAP challenged mice with respect to serum ALT or microRNA-122 (miR-122), a sensitive biomarker for hepatocyte damage (Supplementary Fig. 2A and B). These results indicate that antibody treatments were neither hepatotoxic nor did they alter baseline levels of systemic liver injury markers.

Mice challenged with APAP for 10h demonstrated characteristic hepatic pathophysiological changes as compared to normal mice (Fig 2D and Supplementary Fig. 3). Hepatic tissue expression of HMGB1 was lost in central necrotic areas but upregulated in the periportal areas (Supplementary Fig. 3). In mice challenged with APAP for 10h, the hepatic GSH concentrations dropped from 32.4 ± 6.2 to 5.1 ± 1.9 nmols/mg \pm SD (Fig 2A). A similar decrease in hepatic GSH was seen in all mice treated 2h post-APAP with PBS, E2, m2G7 and h2G7 indicating comparable APAP metabolism between the treatment groups (Fig. 2A). In concordance with previous studies based on antibodies targeting HMGB1 in APAP-challenged mice (7, 15), 2G7 treatments mediated a significant reduction in serum ALT and miR-122 levels compared to the E2 control group (Fig. 2B and C). No significant difference was observed between the m2G7 and h2G7 treatment groups indicating equivalent hepatoprotective properties (Fig. 2B and C). Confirmatory histological results were recorded and revealed reduced tissue destruction and alleviated inflammation in the h2G7 treated mice (Fig.

2D and E). A clear trend in hepato-protection as analyzed by histology was also seen with m2G7 treatment, although this difference was not statistically significant (Fig. 2E). Quantification of Ki-67 stained liver sections revealed that both m2G7 and h2G7 treatment had significantly less proliferating hepatocytes as compared to livers of E2-treated mice (Supplementary Fig. 4), suggesting a decrease in liver regeneration at 10h post-APAP. However, this may be explained by the decrease in liver injury seen in m2G7 and h2G7 treated mice (Figure 2B-E).

Inflammatory mediators are upregulated as a result of the initial toxic hepatocellular injury induced by APAP exposure (26, 27). Both PBS- and E2-treated mice demonstrated a significant increase in serum levels of MCP-1, CXCL-1 and TNF in APAP-exposed mice compared to non-APAP challenged animals (Fig. 2F). Anti-HMGB1 treatments significantly reduced APAP-induced serum levels of MCP-1 and completely abolished the serum levels of CXCL-1 and TNF as compared to the E2 treatment group. We also measured serum levels of IL-1 β and IFN- γ , since both have been reported upregulated after APAP administration (27). However, these cytokines were undetectable in our experiments (data not shown).

Furthermore, studies were conducted to evaluate lowest effective therapeutic dose by administering one and two orders of magnitude less of h2G7 antibody (i.e. 300, 30 or 3 μ g/mouse). A dose-dependent decrease in serum ALT and miR-122 (Fig. 3A and B) was observed. Interestingly, the lowest dose of h2G7 (3 μ g) did not significantly decrease serum levels of ALT or miR-122, but were still able to significantly block APAP-induced inflammation (Fig. 3C). The release of the hepatocyte biomarkers is a combined consequence of direct APAP-mediated toxicity and of the subsequent inflammation.

In order to explore whether the recorded hepato-protection of 2G7 treatment was an effect observed exclusively in inbred mice we also investigated the therapeutic effect of

m2G7 treatment in outbred CD-1 mouse strain. In agreement with the results observed in C57BL/6 mice, m2G7-treated CD-1 animals expressed significantly reduced serum levels of ALT as compared to PBS-treated animals (Fig. 3D). HMGB1-induced inflammatory effects are known to be antagonized by the truncated box A domain of the HMGB1 molecule, by means that are not fully resolved. These therapeutic results have previously been demonstrated in multiple experimental disease models (18, 28, 29), but never before studied in APAP-ALI. A single IP injection of box A showed similar hepato-protective effects as the m2G7 treatment (Fig. 3D), confirming that other strategies for extracellular HMGB1 blockade are also beneficial in APAP-ALI. Injection of box A or m2G7, in non-APAP challenged CD-1 mice, did not alter the levels of hepatic GSH or serum levels of ALT (Supplementary Fig. 4A and B). In line with these observations, a uniform decrease of hepatic GSH was seen in all APAP challenged CD-1 mice regardless of treatment (Supplementary Fig. 5A).

Specific anti-HMGB1 therapy has a delayed therapeutic window as compared to NAC

Post-injury inflammation is highly deleterious in APAP-ALI patients and is especially evident in late-presenting patients where NAC treatment fails to confer hepato-protection. We therefore wanted to investigate whether anti-HMGB1 treatment provided an extended window of therapeutic intervention. APAP challenged mice (300mg/kg) were treated with either NAC, E2 or h2G7 at 2h post-APAP or 6h post- APAP and monitored for 24h. In line with previous reports, NAC treatment at 2h post-APAP completely abrogated the increase in serum ALT (Fig 4A). However, NAC failed to confer hepatoprotection at 6h post-APAP whereas h2G7 treatment was hepatoprotective at both 2h and 6h post-APAP as measured by serum ALT levels (Fig. 4A and B). The reality in the clinic is that all APAP-ALI patients (depending on serum APAP concentration??) receive NAC-treatment and we thus, in addition, investigated the effect of NAC-h2G7 combination treatment. We could not record any beneficial effects of the combination treatments at any time point (Fig. 4A and B), supporting that h2G7 treatment

rather targets the post-injury inflammation than the initial metabolic injury that is counteracted by NAC treatment.

Generation of effector function-deficient h2G7 variants

Immunomodulatory effects of antibody therapies can be mediated via several different mechanisms. Antibodies may block the function of an antigen by binding and neutralizing its target, by activating the classical complement pathway through interaction with C1q or by the engagement of Fcγ receptors (FcγR) and thus inducing cell-mediated effects. In order to outline the therapeutic importance of Fc-mediated effector functions of h2G7 antibody in APAP-ALI, we generated effector function-deficient variants by modifying its CH2 domain either by site-directed-mutagenesis or by endoS treatment, which removes N-linked glycosylation on Fc part of antibodies (30-32). Importantly, none of the Fc-modified variants of h2G7 affected the binding to HMGB1 (data not shown). A lysine-to-alanine mutant variant of h2G7 was generated (K322A), and in contrast to non-modified h2G7, The K322A variant completely abolished binding to human C1q *in vitro* when coated directly (Fig. 5A) or when bound to plates coated with HMGB1 (Fig. 5B). In similarity to the K322A mutant, endoS-treated h2G7 did not bind to C1q (data not shown).

Hydrolysis of the N-linked glycan at position N297 by endoS treatment was verified by a characteristic mass-shift (Fig. 6A) and by a reduced binding to *Lens culinaris* agglutinin (LCA) (Fig. 6B and Supplementary Fig. 6A), which specifically binds to N-linked glycans. To verify that deglycosylation reduced FcR binding we evaluated this binding *in vitro*. Human IgG1 has the capacity to bind and activate all members of the FcγR family and, as predicted, deglycosylation of h2G7 ablated binding to human recombinant FcγRI/CD64 (Fig. 6C and Supplementary Fig. 6B). We further investigated binding of h2G7 to human THP-1 cells that express both CD64 and FcγRII/CD16. The endoS treatment significantly reduced

binding of h2G7 to THP-1 cells (Fig. 6D and Supplementary Fig. 6C). The K322A mutant and non-modified h2G7 displayed similar binding to LCA, CD64 and THP-1 cells (data not shown).

Therapeutic properties of effector function-deficient h2G7

We next studied the therapeutic *in vivo* efficacy of the effector function-deficient h2G7 variants in order to elucidate the mechanism by which h2G7 elicits its hepato-protective and anti-inflammatory effect. Treatment with the modified variant antibodies (K322A and endoS-treated h2G7) and h2G7 in APAP-challenged mice showed similar hepato-protective effects, as determined by a comparable reduction of serum ALT (Fig. 7A) and miR-122 (Supplementary Fig. 7B). Equivalent anti-inflammatory effects, as measured by reduced levels of TNF (Fig. 7B), CXCL-1 (Fig. 7C) and MCP-1 (Fig. 7D), were also recorded. These results collectively establish that the therapeutic effects of h2G7 were mediated via HMGB1 neutralization rather than via complement activation or Fc receptor-mediated effects.

Discussion

APAP is one of the most common over-the-counter drugs and is generally safe at recommended therapeutic doses. Nevertheless, APAP intoxication is a clinical problem and may result in ALI or even death. During clinical APAP overdose, a worse prognosis is correlated with activation of post injury inflammation and systemic inflammatory response syndrome (SIRS) (2, 4, 27, 33). Given the inadequacy of current therapy (i.e. NAC), especially in late-presenting patients, there is a need for development of novel therapies targeting the post-injury inflammation. Specific immune-modulatory therapies are as of yet not available as treatment options for APAP-ALI although such therapeutic strategies would potentially prolong the therapeutic window. Indeed, our data strongly supports that anti-

HMGB1 therapy significantly prolongs the therapeutic window of experimental APAP-ALI (Fig. 3) and would likely be invaluable in treatment of late-presenting patients or in patients that do not respond satisfactory to NAC. HMGB1 has been shown to be a pivotal regulator and biomarker of injury as a result of APAP overdose (2, 10). Therapeutic neutralization of HMGB1 has the potential to improve outcome of several human diseases but no published clinical trials using HMGB1-specific inhibitors have so far been conducted. A paucity of HMGB1 antagonists suitable for the clinic has until now been the major restricting element for further progress. Accordingly, the main purpose of this study was to engineer a chimeric HMGB1-specific mAb with the potential to be evaluated in future clinical trials, by investigating its therapeutic efficacy in a previously shown HMGB1-dependent experimental model of APAP-ALI. We believe that the outcome of our study, the partly humanized h2G7, represents a promising candidate for further clinical exploration.

Conserved proteins are poor immunogens and raising protective therapeutic monoclonal antibodies (mAbs) that target such proteins is a challenging enterprise (34). Hence, generating therapeutically efficient mAbs specific for HMGB1 (99% sequence conservation in mammals) has proven no exception to this experience. It took several years after the original polyclonal anti-HMGB1 antibody treatment study (17) until an anti-HMGB1 mAb (m2G7) was demonstrated to confer experimental disease protection (22, 35). Although a few additional mouse mAbs targeting HMGB1 have mediated successful results in preclinical disease models (36, 37), none has demonstrated comparable universal therapeutic efficacy as the 2G7 mAb that ameliorates diverse inflammatory disease models (Supplementary Table 1). The generated chimeric 2G7 antibody with its replacement of the constant m2G7 frameworks with human sequences may possibly meet the drug development requirements for an HMGB-specific antibody therapy that would be suitable for clinical trials. Humanization processes may alter both specificity and affinity of an antibody (23) and for that reason we investigated

whether a change in the constant immunoglobulin framework modified the *in vitro* properties of 2G7. Our results indicate that h2G7 did not interact with anti-mouse IgG antibodies, implicating that removal of the murine constant frameworks significantly reduced immunogenicity (data not shown) but with preserved antigen-specificity and affinity (Fig. 1B and C).

The therapeutic efficacy of m2G7 in preventing HMGB1-induced sterile inflammation has emphasized the clinical potential of 2G7 in several disorders (Supplementary table 2) and especially in hepatic disorders (7, 35). HMGB1 levels are increased in clinical and experimental APAP-ALI and surpass ALT as a predictor of clinical outcome after APAP intoxication (2, 10). The central functional role of HMGB1 in APAP-ALI pathogenesis is highlighted by the fact that hepatocyte specific abrogation of *Hmgb1* and anti-HMGB1 treatment is highly protective in experimental model APAP-ALI (7, 14). In addition, extensive post-injury inflammation negatively correlates with patient outcome (i.e. need for liver transplant or death). Our results based on therapeutic interventions with h2G7 or m2G7 are in full agreement with this concept and confirm retained functionality of the novel h2G7 antibody. Furthermore, therapeutic intervention with h2G7 is superior to NAC treatment at late time points of experimental APAP-ALI, possibly providing a novel treatment specifically targeting post-injury inflammation with a prolonged therapeutic window of opportunity at which NAC treatment fails to confer hepato-protection.

Recent structural HMGB1 studies emphasize that the redox states of its three conserved cysteine residues regulate the receptor-binding ability and subsequent biological functions. Fully reduced HMGB1 (all-thiol) acts a chemotactic factor, partially oxidized HMGB1 (disulfide) induces cytokines via the TLR4/MD-2, while the fully oxidized HMGB1 (sulfonyl) exerts no demonstrable inflammatory activity (6, 38, 39). All three isoforms are systemically present in APAP challenged mice although at different stages of the post-injury

inflammation (6). HMGB1 isoforms (various redox and acetylated isoforms) are readily detected by 2G7 in immunoblot analysis (data not shown) or by direct-ELISA (Fig 1D and E), but we cannot further comment on conceivable binding preferences of the antibodies to any of the HMGB1 isoforms *in vivo*. It has previously been demonstrated that m2G7 inhibits both HMGB1-induced cytokine production (39) as well as HMGB1-induced cell migration *in vitro* (personal communication with prof. Marco E. Bianchi). Our *in vivo*-based studies further support that h2G7 and m2G7 inhibits HMGB1-driven cytokine and chemokine release in experimental APAP-ALI equally well (Fig. 2F). Likewise, several *in vivo* models of sterile inflammation have demonstrated that m2G7 suppresses both HMGB1-induced migration and cytokine production (Supplementary Table_1). This collectively suggests that 2G7 hampers the effect of both known inflammatory isoforms of HMGB1.

The hepato-protective effects and elimination of inflammatory mediators in response to 2G7 treatment, underline the pathogenic contribution of inflammation in APAP-ALI and that APAP-induced inflammation is highly HMGB1-dependent. A single injection of 3 μ g of h2G7 as well as the hepato-protective dose of 300 μ g completely eliminated the studied circulating inflammatory mediators (Fig. 3). Yang *et al.* demonstrated that treatment with low-dose m2G7 (5 μ g) per mouse at 2h and a repeated dose at 7h post-APAP was both hepato-protective and anti-inflammatory at 24h post-APAP (7). The higher dose required in our study for hepato-protection could possibly be explained by experimental kinetic differences regarding the post-injury inflammatory response or that a single low-dose injection of h2G7 is not sufficient to confer hepato-protection. Nevertheless, the functional similarities of h2G7 and m2G7 in the current study suggest that h2G7 may exert life-saving effects in APAP-induced ALI in a clinical setting.

None of the previous preclinical studies involving m2G7 have addressed the mechanism of action of the m2G7 parental antibody. The present generation of a novel chimeric 2G7

antibody (h2G7) allowed us to, in a controlled manner, modify its effector functions and thus study its mechanism of action. In concurrence with previously published data (40), a K322A substitution of h2G7 completely suppressed C1q binding without affecting binding to FcγRs. The aglycosylated h2G7 was incapable of binding neither C1q nor FcγRs. Since deglycosylation of antibodies may affect binding to C1q it is important to recognize both isotype- and species-specific differences especially when conducting studies comparing therapeutic antibodies (31, 32, 41). The binding of aglycosylated mouse IgG2b to C1q is negligible and it is therefore likely that endoS-treated m2G7 would have the same effect (42). Our *in vivo* data collectively suggest that h2G7 acts through antigen neutralization rather than complement activation or FcγR engagement, since neither the K322A mutant nor endoS-treated h2G7 displayed altered therapeutic activity as compared to non-modified h2G7. The *in vivo* neutralizing effects of 2G7 could possibly be explained by a direct steric blocking of HMGB1-receptor interaction. As shown for other therapeutic antibodies, it is conceivable that a competition for receptor binding sites is sufficient for the observed HMGB1 neutralization by h2G7 or that allosteric mechanisms induce or suppress conformational changes thus altering the function of HMGB1 (43). Further in-depth studies are required to define whether h2G7 has a preference for certain HMGB1 isoforms and to elucidate the detailed mechanisms for h2G7-mediated neutralization.

To summarize, we here report the creation of a partly humanized, chimeric mAb targeting HMGB1 with preserved functionality compared to the parental mouse anti-HMGB1 mAb. We conclude that HMGB1 neutralization was the observed mechanism of action in experimental APAP-ALI. The h2G7 antibody would likely provide significant advantages in a clinical setting due to reduced xenogeneic immune responses and improved pharmacokinetics as compared to mouse anti-HMGB1 mAbs, especially in late-presenting patients and in patients

1
2
3
4
5
6
7
8
9
10
11
12
13
14
15
16
17
18
19
20
21
22
23
24
25
26
27
28
29
30
31
32
33
34
35
36
37
38
39
40
41
42
43
44
45
46
47
48
49
50
51
52
53
54
55
56
57
58
59
60

with a need for repeated treatment. These results provide distinct progress in the endeavor to bring an HMGB1-specific antagonist to further clinical development.

For Peer Review

Acknowledgement

We thank Tomas Nyman for technical assistance with SPR studies and Sophie Regan, Jack Sharkey and Alison Rodrigues for assistance with the *in vivo* studies.

For Peer Review

References

1. Watkins PB, Merz M, Avigan MI, Kaplowitz N, Regev A, Senior JR. The clinical liver safety assessment best practices workshop: rationale, goals, accomplishments and the future. *Drug Saf* 2014;37 Suppl 1:S1-7.

2. Antoine DJ, Jenkins RE, Dear JW, Williams DP, McGill MR, Sharpe MR, Craig DG, et al. Molecular forms of HMGB1 and keratin-18 as mechanistic biomarkers for mode of cell death and prognosis during clinical acetaminophen hepatotoxicity. *J Hepatol* 2012;56:1070-1079.

3. Ostapowicz G, Fontana RJ, Schiodt FV, Larson A, Davern TJ, Han SH, McCashland TM, et al. Results of a prospective study of acute liver failure at 17 tertiary care centers in the United States. *Ann Intern Med* 2002;137:947-954.

4. Antoniadou CG, Quaglia A, Taams LS, Mitry RR, Hussain M, Abeles R, Possamai LA, et al. Source and characterization of hepatic macrophages in acetaminophen-induced acute liver failure in humans. *Hepatology* 2012;56:735-746.

5. Schiraldi M, Raucci A, Munoz LM, Livoti E, Celona B, Venereau E, Apuzzo T, et al. HMGB1 promotes recruitment of inflammatory cells to damaged tissues by forming a complex with CXCL12 and signaling via CXCR4. *J Exp Med* 2012;209:551-563.

6. Yang H, Lundback P, Ottosson L, Erlandsson-Harris H, Venereau E, Bianchi ME, Al-Abed Y, et al. Redox modification of cysteine residues regulates the cytokine activity of high mobility group box-1 (HMGB1). *Mol Med* 2012;18:250-259.

7. Yang H, Wang H, Ju Z, Ragab AA, Lundback P, Long W, Valdes-Ferrer SI, et al. MD-2 is required for disulfide HMGB1-dependent TLR4 signaling. *J Exp Med* 2015.

8. Kang R, Chen R, Zhang Q, Hou W, Wu S, Cao L, Huang J, et al. HMGB1 in health and disease. *Mol Aspects Med* 2014;40:1-116.

9. Bonaldi T, Talamo F, Scaffidi P, Ferrera D, Porto A, Bachi A, Rubartelli A, et al. Monocytic cells hyperacetylate chromatin protein HMGB1 to redirect it towards secretion. *EMBO J* 2003;22:5551-5560.

10. Antoine DJ, Dear JW, Lewis PS, Platt V, Coyle J, Masson M, Thanacoody RH, et al. Mechanistic biomarkers provide early and sensitive detection of acetaminophen-induced acute liver injury at first presentation to hospital. *Hepatology* 2013;58:777-787.

11. Yang M, Antoine DJ, Weemhoff JL, Jenkins RE, Farhood A, Park BK, Jaeschke H. Biomarkers distinguish apoptotic and necrotic cell death during hepatic ischemia/reperfusion injury in mice. *Liver Transpl* 2014;20:1372-1382.

12. Ge X, Antoine DJ, Lu Y, Arriazu E, Leung TM, Klepper AL, Branch AD, et al. High mobility group box-1 (HMGB1) participates in the pathogenesis of alcoholic liver disease (ALD). *J Biol Chem* 2014;289:22672-22691.

13. Woolbright BL, Dorko K, Antoine DJ, Clarke JL, Gholami P, Li F, Kumer SC, et al. Bile acid-induced necrosis in primary human hepatocytes and in patients with obstructive cholestasis. *Toxicol Appl Pharmacol* 2015;283:168-177.

14. Huebener P, Pradere J, Hernandez C, Gwak G, Caviglia JM, Mu X, Loike JD, et al. The HMGB1/RAGE axis triggers neutrophil-mediated injury amplification following necrosis. *J Clin Invest* 2014.

15. Antoine DJ, Williams DP, Kipar A, Lavery H, Park BK. Diet restriction inhibits apoptosis and HMGB1 oxidation and promotes inflammatory cell recruitment during acetaminophen hepatotoxicity. Mol Med 2010;16:479-490.
16. Andersson U, Tracey KJ. HMGB1 Is a Therapeutic Target for Sterile Inflammation and Infection. Annual Review of Immunology, Vol 29 2011;29:139-162.
17. Wang H, Bloom O, Zhang M, Vishnubhakat JM, Ombrellino M, Che J, Frazier A, et al. HMG-1 as a late mediator of endotoxin lethality in mice. Science 1999;285:248-251.
18. Kokkola R, Li J, Sundberg E, Aveberger AC, Palmblad K, Yang H, Tracey KJ, et al. Successful treatment of collagen-induced arthritis in mice and rats by targeting extracellular high mobility group box chromosomal protein 1 activity. Arthritis Rheum 2003;48:2052-2058.
19. Knezevic I, Kang HN, Thorpe R. Immunogenicity assessment of monoclonal antibody products: A simulated case study correlating antibody induction with clinical outcomes. Biologicals 2015;43:307-317.
20. Amara K, Steen J, Murray F, Morbach H, Fernandez-Rodriguez BM, Joshua V, Engstrom M, et al. Monoclonal IgG antibodies generated from joint-derived B cells of RA patients have a strong bias toward citrullinated autoantigen recognition. J Exp Med 2013;210:445-455.
21. Tiller T, Meffre E, Yurasov S, Tsuiji M, Nussenzweig MC, Wardemann H. Efficient generation of monoclonal antibodies from single human B cells by single cell RT-PCR and expression vector cloning. J Immunol Methods 2008;329:112-124.
22. Qin S, Wang H, Yuan R, Li H, Ochani M, Ochani K, Rosas-Ballina M, et al. Role of HMGB1 in apoptosis-mediated sepsis lethality. J Exp Med 2006;203:1637-1642.
23. McLean GR, Torres M, Elgueabal N, Nakouzi A, Casadevall A. Isotype can affect the fine specificity of an antibody for a polysaccharide antigen. J Immunol 2002;169:1379-1386.
24. Scaffidi P, Misteli T, Bianchi ME. Release of chromatin protein HMGB1 by necrotic cells triggers inflammation. Nature 2002;418:191-195.
25. Yang R, Zou X, Tenhunen J, Zhu S, Kajander H, Koskinen ML, Tonnessen TI. HMGB1 neutralization is associated with bacterial translocation during acetaminophen hepatotoxicity. BMC Gastroenterol 2014;14:66.
26. Lawson JA, Farhood A, Hopper RD, Bajt ML, Jaeschke H. The hepatic inflammatory response after acetaminophen overdose: role of neutrophils. Toxicol Sci 2000;54:509-516.
27. Jaeschke H, Williams CD, Ramachandran A, Bajt ML. Acetaminophen hepatotoxicity and repair: the role of sterile inflammation and innate immunity. Liver Int 2012;32:8-20.
28. Gong Q, Xu JF, Yin H, Liu SF, Duan LH, Bian ZL. Protective effect of antagonist of high-mobility group box 1 on lipopolysaccharide-induced acute lung injury in mice. Scand J Immunol 2009;69:29-35.
29. Yang H, Ochani M, Li J, Qiang X, Tanovic M, Harris HE, Susarla SM, et al. Reversing established sepsis with antagonists of endogenous high-mobility group box 1. Proc Natl Acad Sci U S A 2004;101:296-301.
30. Duncan AR, Winter G. The binding site for C1q on IgG. Nature 1988;332:738-740.

31. Nandakumar KS, Collin M, Olsen A, Nimmerjahn F, Blom AM, Ravetch JV, Holmdahl R. Endoglycosidase treatment abrogates IgG arthritogenicity: importance of IgG glycosylation in arthritis. Eur J Immunol 2007;37:2973-2982.

32. Allhorn M, Briceno JG, Baudino L, Lood C, Olsson ML, Izui S, Collin M. The IgG-specific endoglycosidase EndoS inhibits both cellular and complement-mediated autoimmune hemolysis. Blood 2010;115:5080-5088.

33. Stutchfield BM, Antoine DJ, Mackinnon AC, Gow DJ, Bain CC, Hawley CA, Hughes MJ, et al. CSF1 Restores Innate Immunity After Liver Injury in Mice and Serum Levels Indicate Outcomes of Patients With Acute Liver Failure. Gastroenterology 2015;149:1896-1909 e1814.

34. Sinclair NR. B cell/antibody tolerance to our own antigens. Front Biosci 2004;9:3019-3028.

35. Tsung A, Sahai R, Tanaka H, Nakao A, Fink MP, Lotze MT, Yang H, et al. The nuclear factor HMGB1 mediates hepatic injury after murine liver ischemia-reperfusion. J Exp Med 2005;201:1135-1143.

36. Liu K, Mori S, Takahashi HK, Tomono Y, Wake H, Kanke T, Sato Y, et al. Anti-high mobility group box 1 monoclonal antibody ameliorates brain infarction induced by transient ischemia in rats. FASEB J 2007;21:3904-3916.

37. Zhang F, Huang G, Hu B, Fang LP, Cao EH, Xin XF, Song Y, et al. Anti-HMGB1 neutralizing antibody ameliorates neutrophilic airway inflammation by suppressing dendritic cell-mediated Th17 polarization. Mediators Inflamm 2014;2014:257930.

38. Venereau E, Casalgrandi M, Schiraldi M, Antoine DJ, Cattaneo A, De Marchis F, Liu J, et al. Mutually exclusive redox forms of HMGB1 promote cell recruitment or proinflammatory cytokine release. J Exp Med 2012;209:1519-1528.

39. Yang H, Hreggvidsdottir HS, Palmblad K, Wang H, Ochani M, Li J, Lu B, et al. A critical cysteine is required for HMGB1 binding to Toll-like receptor 4 and activation of macrophage cytokine release. Proc Natl Acad Sci U S A 2010;107:11942-11947.

40. Idusogie EE, Presta LG, Gazzano-Santoro H, Totpal K, Wong PY, Ultsch M, Meng YG, et al. Mapping of the C1q binding site on rituxan, a chimeric antibody with a human IgG1 Fc. J Immunol 2000;164:4178-4184.

41. **Benkhoucha M, Molnarfi N**, Santiago-Raber ML, Weber MS, Merkler D, Collin M, Lalive PH. IgG glycan hydrolysis by EndoS inhibits experimental autoimmune encephalomyelitis. J Neuroinflammation 2012;9:209.

42. Nose M, Wigzell H. Biological significance of carbohydrate chains on monoclonal antibodies. Proc Natl Acad Sci U S A 1983;80:6632-6636.

43. Bhaskar V, Goldfine ID, Bedinger DH, Lau A, Kuan HF, Gross LM, Handa M, et al. A fully human, allosteric monoclonal antibody that activates the insulin receptor and improves glycemic control. Diabetes 2012;61:1263-1271.

Author names in bold designate shared co-first authorship

Figure legends

Figure 1.

Chimeric anti-HMGB1 antibody has retained specificity and affinity as its murine analog. (A) Constant and variable domain comparison of the parental mAb m2G7 and the chimeric h2G7 antibody denoted with known key residues regulating antibody effector functions. (B) Antigen specificity was tested by direct-ELISA. HMGB1 (left), box A (middle) or box B (right) was coated on plates and incubated with antibodies at increasing concentration. h2G7 (green) and m2G7 (red) displayed similar antigen specificity by binding to both HMGB1 and the box A domain but not to box B. The control human IgG1 antibody E2 (black) did not display binding to any of the proteins. (C) SPR analysis was performed to define binding affinities to HMGB1. Antibodies were immobilized on a CM5-dextran chip and HMGB1 was injected at various concentrations (55, 100, 220, 440 or 880nM). h2G7 displayed slightly higher affinity (left, $K_d = 130\text{nM}$) towards HMGB1 as compared to m2G7 (middle, $K_d = 170\text{nM}$). No signal was detected from the E2 channel (right). (D-E) Indicated redox isoforms of HMGB1 were coated and (D) m2G7 or (E) h2G7 were added at increasing concentrations and detected with anti-mouse IgG or anti-human IgG, respectively.

Figure 2.

Similar therapeutic efficacy of h2G7 and m2G7 following APAP-ALI. Fasted C57BL/6 mice were subjected to 530mg/kg of APAP. PBS, 300 μg m2G7, h2G7 or IgG1 control antibody (E2) was administered at 2h post-APAP (n=6). At 10h post-APAP, (A) Hepatic GSH, (B) serum ALT (C) serum miR-122 expression, (D) representative histological sections (H&E stainings) and (E) histological score were analyzed to evaluate hepatic injury. Levels of the inflammatory mediators (F) TNF, CXCL-1 and MCP-1 in serum were quantified. If

undetectable, values were substituted with the lowest limit of detection (50pg/mL). Data is presented as means±SEM. * = $P < 0.05$ and ** = $P < 0.01$ by Kruskal-Wallis with Dunns post-test.

Figure 3.

Dose-dependent hepato-protection and completely abolished inflammation with anti-HMGB1 therapy. (A-C) APAP-challenged C57BL/6 mice (530mg/kg) were treated (2h post-APAP) with h2G7 (3, 30 and 300µg/mouse) or with 300µg E2 ctrl antibody (n=6). Serum levels of (A) ALT and (B) miR-122 indicate a dose dependent hepato-protection with h2G7 as treatment and a complete abrogation of (C) inflammatory mediators, independent of therapeutic dose. (D) Serum ALT levels in APAP-challenged CD-1 mice (530mg/kg) treated (2h post-APAP) with PBS, 300µg m2G7 or 300µg box A for 10h (n = 7). If undetectable, values were substituted with the lowest limit of detection (50pg/mL). Data is presented as mean±SEM. * = $P < 0.05$, ** = $P < 0.01$, and *** = $P < 0.001$ by Kruskal-Wallis with Dunns post-test.

Figure 4.

Targeting post-injury inflammation with h2G7 prolongs the therapeutic window of opportunity compared to NAC treatment. APAP-challenged C57BL/6 mice (300mg/kg) were treated (A) 2h or (B) 6h post-APAP with h2G7 (300µg/mouse), 300µg E2 ctrl antibody (300µg/mouse) or NAC (/mouse) alone or in combination (n=10) and sacrificed at 24h post-APAP. Hepato-protection was recorded as a decrease in serum ALT levels. Data is presented as mean±SEM. * = $P < 0.05$, ** = $P < 0.01$, and *** = $P < 0.001$ by Kruskal-Wallis with Dunn's post-test.

Figure 5.

Abrogated binding to complement C1q *in vitro* by a K322A mutation. Plates were coated with indicated antibodies directly or with HMGB1. (A) Deposition of C1q from normal human sera (NHS) on plates coated with K322A or h2G7. Human serum albumin (HSA) or aggregated human IgG (Agg.IgG) were used as negative and positive controls, respectively. (B) K322A did not bind to C1q when complexed with HMGB1. In experiments with HMGB1 coating, data were normalized towards the h2G7 signal at 1% NHS which was set as 100% C1q deposition. Results are represented as means \pm SEM from three independent experiments.

Figure 6.

Aglycosylated h2G7 display reduced binding to Fc receptors *in vitro*. Deglycosylation of h2G7 was performed by endoS treatment and was analyzed by (A) reducing SDS-PAGE. A small decrease in mass indicated deglycosylation of the IgG γ chain. (B) *Lens culinaris* agglutinin (LCA) displayed significantly reduced binding to plates coated with endoS-treated h2G7 as compared to non-treated h2G7. (C) EndoS treatment of h2G7 significantly reduced human recombinant CD64. (D) Binding to live THP-1 cells incubated with PBS, h2G7 or endoS-treated h2G7. Results are represented as means \pm SEM from three independent experiments. *** = $P < 0.001$ by one-way ANOVA with Bonferroni post-test.

Figure 7.

Effector-function deficient h2G7 variants demonstrate analogous therapeutic effects as h2G7. APAP-exposed C57BL/6 mice (530mg/kg) were treated with 300 μ g E2, K322A, endoS-treated h2G7 or h2G7 at 2h post-APAP (n = 6). (A) K322A, endoS-treated h2G7 and h2G7 demonstrate equivalent hepato-protective effects as measured by serum ALT. No significant difference was noted between the h2G7 treatment groups (gray bars) with respect to anti-

1
2
3
4
5
6
7
8
9
10
11
12
13
14
15
16
17
18
19
20
21
22
23
24
25
26
27
28
29
30
31
32
33
34
35
36
37
38
39
40
41
42
43
44
45
46
47
48
49
50
51
52
53
54
55
56
57
58
59
60

inflammatory activity as measured by a decrease in (B) TNF, (C) CXCL-1 or (D) MCP-1.
Undetectable levels were substituted with the value for lowest limit of detection (50pg/mL).
Data is presented as means±SEM. ** = $P < 0.01$, and *** = $P < 0.001$ by Kruskal-Wallis with
Dunn's post-test.

For Peer Review

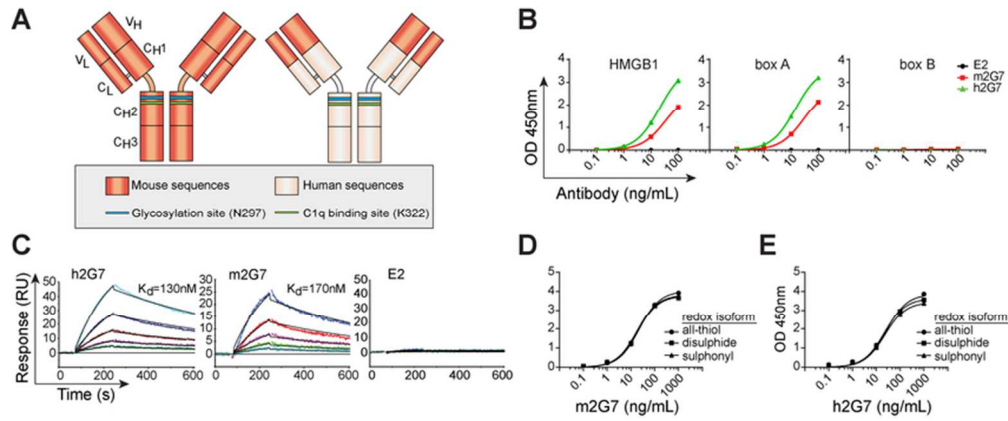


Figure 1
71x29mm (300 x 300 DPI)

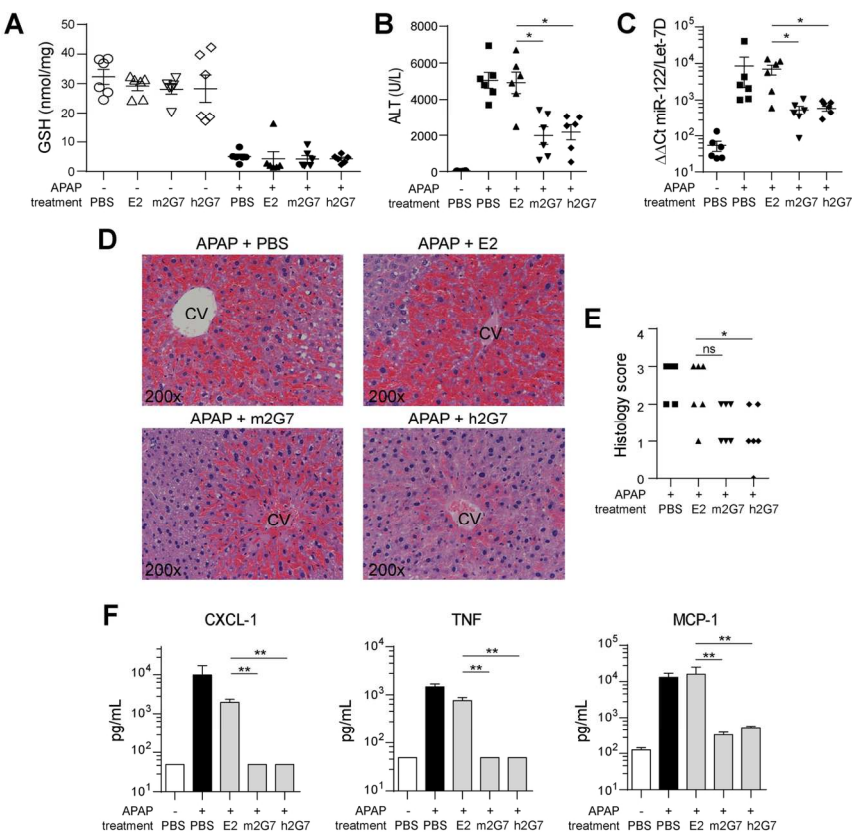


Figure 2
143x117mm (300 x 300 DPI)

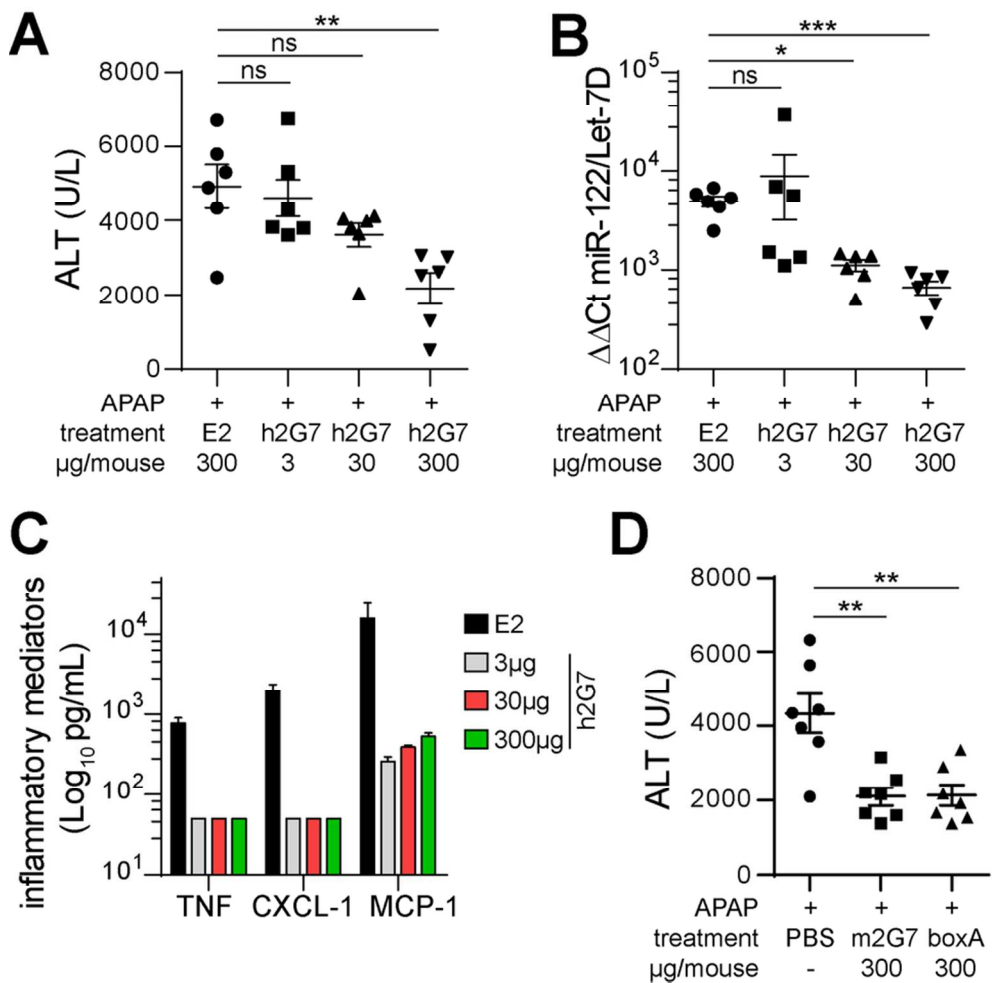


Figure 3
82x80mm (300 x 300 DPI)

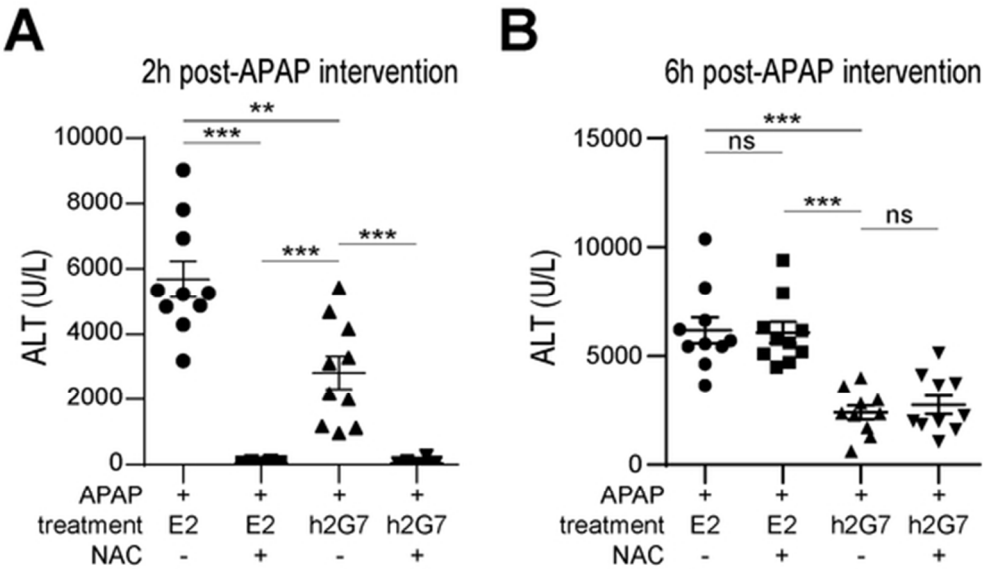


Figure 4
49x29mm (300 x 300 DPI)

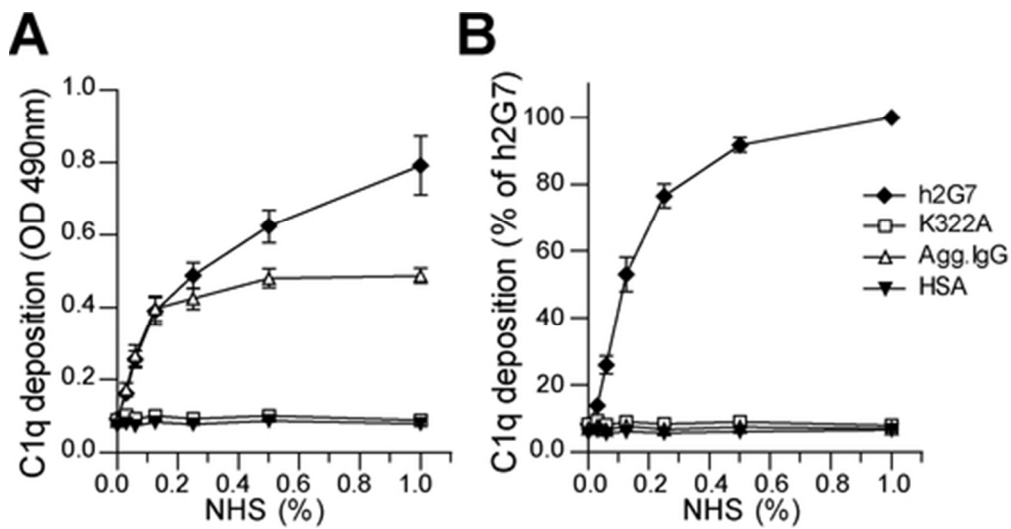


Figure 5
44x23mm (300 x 300 DPI)

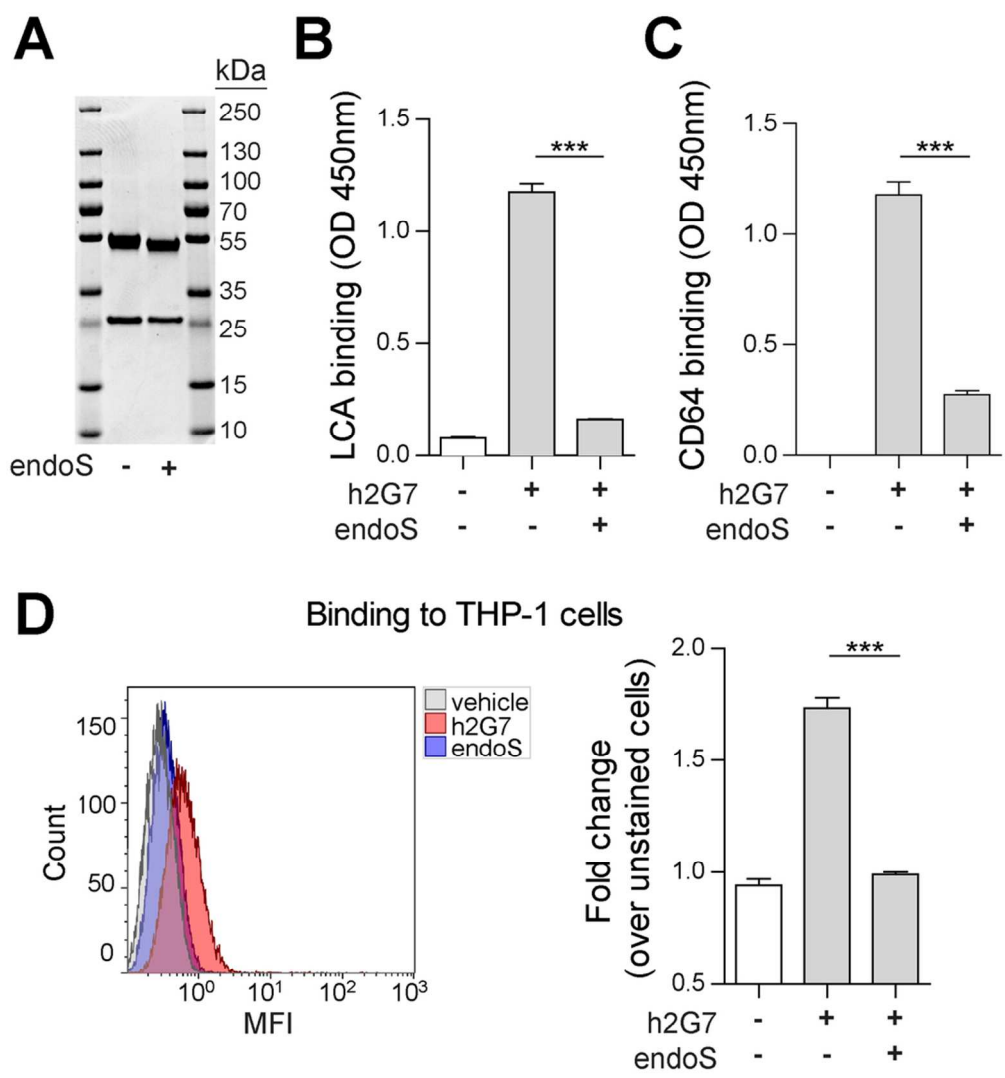


Figure 6
90x97mm (300 x 300 DPI)

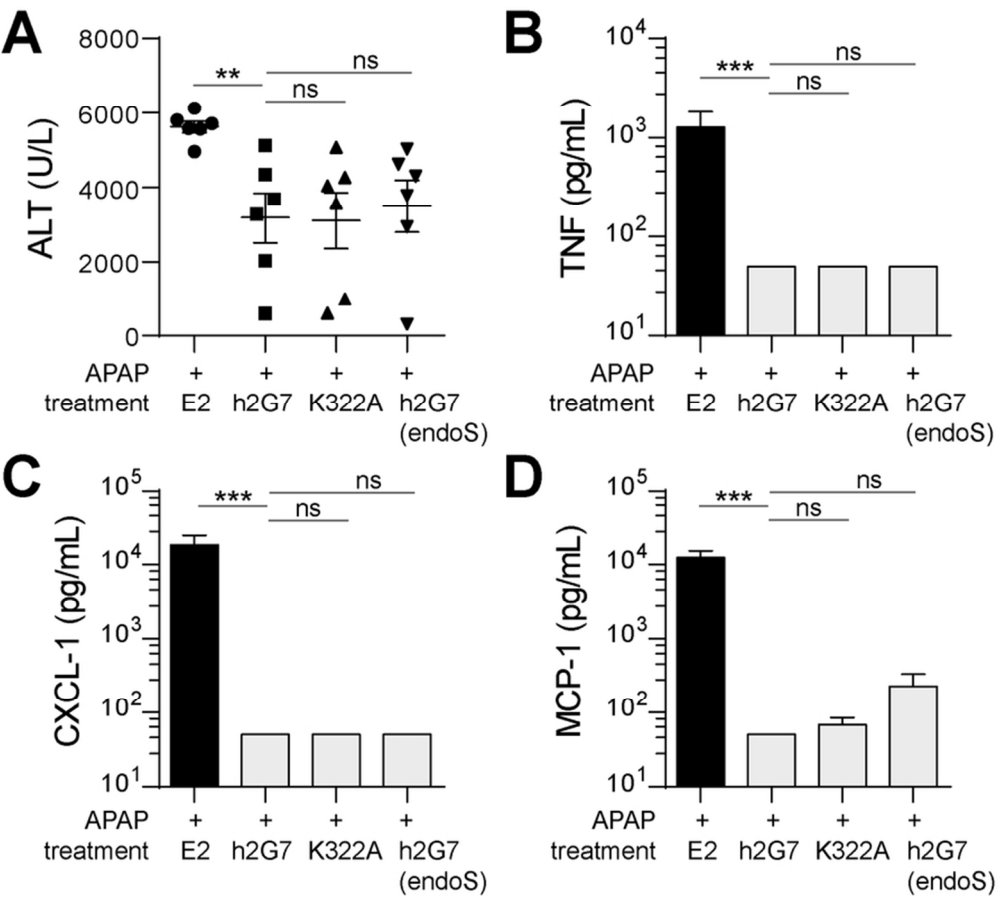


Figure 7
75x67mm (300 x 300 DPI)

1
2
3
4
5
6
7
8
9
10
11
12
13
14
15
16
17
18
19
20
21
22
23
24
25
26
27
28
29
30
31
32
33
34
35
36
37
38
39
40
41
42
43
44
45
46
47
48
49
50
51
52
53
54
55
56
57
58
59
60

Supplementary data to:

A novel HMGB1 neutralizing chimeric antibody attenuates DILI and post-injury
inflammation

Peter Lundbäck¹, Jonathan D. Lea², Agnieszka Sowinska¹, Lars Ottosson³, Camilla
Melin Fürst⁴, Johanna Steen¹, Cecilia Aulin¹, Joanna I. Clarke², Anja Kipar², Lena
Klevenvall³, Huan Yang⁵, Karin Palmblad³, B. Kevin Park², Kevin J. Tracey⁵, Anna
M. Blom⁴, Ulf Andersson³, Daniel J. Antoine^{2,#}, and Helena Erlandsson Harris^{1,#}

Supplementary methods

Cloning and protein purification

HMGB1, boxA and boxB cloning and production

All PCR reactions were performed by using Accuprime *pfx* (Life-technologies,
Carlsbad, CA) according to manufacturer’s instructions unless otherwise stated.

HMGB1 cDNA was cloned into a pet28c vector (Novagen) in order to generate
c-terminal 6xHIS-tagged proteins. Primers (Eurofins DNA) used used to amplify
cDNA fragments of HMGB1 are stated in SI Table2. Restrictions enzymes used for
linearization of vector and cleavage of PCR fragment were NcoI and XhoI
(Fermentas). Linearized vectors were treated with shrimp alkaline phosphatase before
insertion of cleaved PCR fragments and ligation with T4 DNA ligase (Fermentas).
Newly generated plasmids were transformed into Oneshot DH5α competent bacteria
(Life Technologies) by a 30sec, 42°C heat pulse. Kanamycin was used as antibiotic
for plasmid selection. For recombinant protein production, plasmids were transformed
into BL-21DE3 bacteria (Life-technologies) and expression was induced by addition
of 1mM IPTG for 16h at room temperature. Bacteria were lyzed in buffer A

(imidazole 20mM and 500mM NaCl) by 4x30sec sonication on ice. Lysate was cleared from debris by centrifugation at 15,000g. Recombinant protein purifications were performed on an ÄKTA Explorer 10 system according to manufacturer's instructions and all buffers used were filtered (0.2µm) and degased before use. Briefly, a HIS-TRAP FF column was equilibrated with 5 column volumes of buffer A before injection of bacterial lysate. The column was washed with increasing concentrations of imidazole (up to 80mM) and protein was eluted with 200mM imidazole and 500mM NaCl. High purity fractions were pooled and the final product was >95% pure. Protein preparations were extensively dialyzed against PBS.

Generation of a chimeric anti-HMGB1 antibody

Cloning was performed as previously described [1, 2]. RNA from hybridoma cells producing monoclonal m2G7 antibodies was isolated by RNeasy columns (Qiagen). Superscript (Life-Technologies) was used to synthesize cDNA. IgGγ and IgGκ variable regions were amplified separately starting from 4µL of cDNA as template with primers stated in SI. Table2. Each round of PCR (50 cycles) was 94°C for 30sec, 58°C for 30sec, and 72°C for 45sec. PCR products were purified using QIAquick PCR purification kit (Qiagen) and digested with restriction enzymes stated in SI. Table2 (New England Biolabs). Digested products were ligated using the quick ligase kit (New England Biolabs) into expression vectors containing the human IgGγ and IgGκ constant regions. Constructs were transformed into DH5α (Invitrogen) and propagated plasmids were isolated with NucleoSpin plasmid DNA isolation kit (Macherey-Nagel). IgGγ and IgGκ plasmids were sequenced (Eurofins DNA) to confirm identity and correct reading frames with the original m2G7 variable region. The irrelevant IgG1 isotype control antibody E2 has specificity towards tetanus toxin and was originally published as 1362SF-E02 [2].

1
2
3
4
5
6
7
8
9
10
11
12
13
14
15
16
17
18
19
20
21
22
23
24
25
26
27
28
29
30
31
32
33
34
35
36
37
38
39
40
41
42
43
44
45
46
47
48
49
50
51
52
53
54
55
56
57
58
59
60

Recombinant antibodies were produced by transient transfection of FreeStyle HEK-293F cells (Gibco, Life Technologies). Cells were cultured at 37°C with 8% CO₂ in FreeStyle 293 Expression medium (Gibco, Life Technologies) to a density of 0.6-0.7x10⁶ cells/mL. The cells were then transfected with 0.5µg of vector DNA for each antibody chain (heavy and light) per mL of cell culture, using the PEI-Max transfection reagent (Polysciences) dissolved in OPTI-PRO SFM medium (Gibco, Life Technologies). Supernatants were collected at 9-10 days post-transfection and antibodies were purified on HiTrap Protein G HP columns (GE Healthcare) using an ÄKTA Explorer 10 system (GE Healthcare). PBS was used as running buffer and the antibodies were eluted with 0.1M glycine (pH 2.7) and neutralized with a suitable amount of 1M Tris buffer (pH 9.0). Antibodies were extensively purified against PBS and concentrations were determined by Nanodrop ND-1000 (Thermo Scientific), and the purity (>98%) of the expressed antibodies was determined by SDS-PAGE .

Generation of K322A mutant

An 18-cycle PCR reaction was performed with h2G7 IgGγ plasmid as template with primers stated in SI. Table2. After PCR-cycling, template DNA was digested by DpnI digestion for 1h at 37°C. PCR produced plasmids were purified by gel extraction and sequenced in order to verify the expected codon change (AAG/GCG).

Antibody specificity testing

1µg HMGB1, box A or box B was coated in an ELISA microtiter plate (Nunc maxisorp) at room temperature overnight. Plates were blocked in 1% BSA in PBS (pH 7.4) for 1h at room temperature. Wash steps were performed with 3x PBS-Tween (0.05%). h2G7, m2G7, K322 or E2 was diluted (100, 10, 1 and 0.1 ng/mL) in antibody diluent (0.1% BSA, 0.05% Tween-20 in tris-buffered saline, pH 7.4) and

incubated at room temperature for 2h. Anti-human or anti-mouse IgG was diluted to 1:10000 in antibody diluent and incubated for 1h at room temperature. 3,3',5,5'-tetramethylbenzidine (TMB) substrate was added and stopped after 5min with 2N sulphuric acid. Optical density at 450nm was determined (with subtraction of plate blank).

Surface plasmon resonance (SPR) kinetic experiments

Kinetic experiments were performed on a Biacore 2000 system (GE Healthcare, Uppsala, Sweden) according to manufacturer's instructions unless otherwise stated. All buffers and samples were 0.2 μ M filtered and degassed prior to use and the Biacore system was primed with running buffer (PBS-T 0.01%). **Immobilization;** Immobilization pH scouting was performed for the h2G7 antibody and the identified optimal settings were adapted for all antibodies. Antibodies were diluted in 10mM sodium acetate, pH 5.0, and immobilized on a CM5 sensor chip by amine coupling using *N*-hydroxysuccimide (NHS) and *N*-ethyl-N-(3-dimethylaminopropyl)-carbodiimide hydrochloride (EDC). Target level for ligand immobilization (R_L) was calculated and set to 600 in order to achieve a theoretical R_{max} of 200. Flow channel 1 (Fc1) was used as reference surface (blank), Fc2 was immobilized with E2, Fc3 with h2G7 and Fc4 with m2G7 antibody. Reactive esters that were not cross-linked were blocked with ethanolamine and 50mM NaOH was used as wash buffer after immobilization. **Kinetic analysis;** A two-fold serial dilution of the analyte HMGB1 was performed (880nM, 440nM, 220nM, 110nM, 55nM and 0nM) in PBS-T. Experiments were performed in direct binding mode at a 30 μ L/min flow rate at 25°C and injection time for HMGB1 (sorted low to high concentration) was 3min followed by a dissociation time of 15min before regeneration with two 45sec pulses of regeneration buffer (10mM Glycine-HCl pH 2.0, 1M NaCl). Stabilization time after

1
2
3
4
5
6
7
8
9
10
11
12
13
14
15
16
17
18
19
20
21
22
23
24
25
26
27
28
29
30
31
32
33
34
35
36
37
38
39
40
41
42
43
44
45
46
47
48
49
50
51
52
53
54
55
56
57
58
59
60

every regeneration buffer injection was set to 2min. **Data analysis;** Data was evaluated using BiaEvaluation. Unnecessary data was subtracted and baselines were adjusted to zero. For each HMGB1 concentration injected, the reference surface signal from Fc1 was subtracted from the other channels (i.e. Fc2-Fc1, Fc3-Fc1 and Fc4-Fc1). The binding curves were also blank-run subtracted by removing the 0nM signal for all concentrations. Curve fitting was done by simultaneous K_a/K_d analysis (1:1 Langmuir binding) and a $\chi^2/R_{max} < 1\%$ was considered as a good fit.

Redox isoform specificity

1 μ g disulfide HMGB1 (HMGBiotech, Milano, Italy) was coated for 16h at 4°C in microtiter plates in 5mM DTT, PBS or 10mM H₂O₂ to generate all-thiol, disulfide or sulphonyl HMGB1. Plates were blocked with 1% BSA for 1h. Increasing concentrations of m2G7 or h2G7 (0.1 – 1000 ng/mL) was added and incubated for 2h at room temperature. Bound antibodies were detected with either HRP-coupled anti-mouse IgG (Sigma-Aldrich, A3854) or anti-human IgG (DAKO Cytomation, Glostrup, Denmark, P0214)

Effector function validations assays

Deglycosylation of h2G7 was performed using deGlycIT columns (Genovis, Lund, Sweden) according to manufacturer’s instructions.

Gelshift assay; 3.75 μ g antibody was subjected to SDS-PAGE on tris glycine 4-20% gradient gels (BioRad). Gel was stained with Coomassie blue and destained in 10% acetic acid and 40% methanol. Deglycosylation effect was verified by a small mass-shift decrease for IgG γ .

***Lens Culinaris* Agglutinin (LCA) binding assay;** Half-area microtiter ELISA plates (Corning) were coated with antibodies at 37°C for 2h. Between each step after coating, plates were thoroughly washed 5x with wash buffer (0.1% TBS-T) and

1
2
3 blocked in wash buffer for 1h at room temperature. Equilibration of plates were
4
5 performed by 5x washes with TC buffer (1mM Tris pH 7.5, 1mM CaCl₂, MgCl₂,
6
7 MnCl₂ and 0.1% Tween). Biotinylated LCA (Vector Labs) was diluted to 1µg/mL in
8
9 TC buffer and added to plates for 1h at 37°C. Streptavidin-HRP was diluted in 0.1%
10
11 TBS-T and incubated for 20min at room temperature. The reaction was started by
12
13 addition of TMB substrate solution and stopped with 2N sulphuric acid.
14
15

16 **CD64 binding assay;** Human recombinant FcγRI/CD64 (Life Technologies) was
17
18 diluted to 1µg/mL in PBS and coated in a half-area microtiter ELISA plates (Corning)
19
20 at 37°C for 2h. Plate was washed 3x with PBS-T (0.05%) between each of the
21
22 following step. Plate was blocked in 1% BSA in PBS for 1h at room temperature.
23
24 Antibodies were diluted in antibody diluent (0.1% BSA, 0.05% Tween-20 in tris-
25
26 buffered saline) and added to the plate for 1.5h at room temperature. Rabbit F(ab')₂
27
28 anti-human (DAKO Cytomation, P0406) was diluted 1:800 in antibody diluent and
29
30 incubated for 45min at room temperature. Reaction was started by addition of TMB
31
32 and stopped with 2N sulphuric acid.
33
34
35

36 **THP-1 binding assay;** THP-1 cells were incubated with antibodies at different
37
38 concentrations for 1h at room-temperature. Bound antibodies were visualized by
39
40 addition of a rabbit F(ab')₂ anti-human (DAKO Cytomation, F0315) as recommended
41
42 by manufacturer. All cell and antibody dilutions were made in PBS supplemented
43
44 with 2% FBS. Mean fluorescence intensity was determined by a Gallios flow
45
46 cytometer (Beckman-Coulter). Data was analyzed by Kaluza Analysis Software.
47
48

49 **Activation of complement by antibodies specific to HMGB1;** Microtiter plates
50
51 (Maxisorp, Nunc) were coated with 5µg/mL of antibodies and controls (human serum
52
53 albumin (HSA) and aggregated human IgG), diluted in PBS for 2h at 37°C. Between
54
55 each incubation step, wells were washed 4x with immunowash (50mM Tris-HCl pH
56
57
58
59
60

1
2
3
4
5
6
7
8
9
10
11
12
13
14
15
16
17
18
19
20
21
22
23
24
25
26
27
28
29
30
31
32
33
34
35
36
37
38
39
40
41
42
43
44
45
46
47
48
49
50
51
52
53
54
55
56
57
58
59
60

8.0, 150mM NaCl, 0.1% Tween-20). After blocking the wells with 1% BSA in PBS for 1h at 37°C, wells were incubated with increasing amounts of normal human serum (NHS) diluted in GVB²⁺ (5mM veronal buffer pH 7.4, 144mM NaCl, 1mM MgCl₂, 0.15mM CaCl₂, and 1% gelatin) for 45min at 37°C. Deposited C1q was detected with specific antibodies (DAKO, A0136) followed by HRP-conjugated secondary antibodies (DAKO, P0399). The plates were developed with o-phenylenediamine (OPD) substrate (DAKO) and H₂O₂ and the absorbance at 490 nm was measured.

Binding of specific antibodies to HMGB1 and activation of complement;
Microtiter plates (Maxisorp, Nunc) were coated with 5µg/mL HMGB1 in PBS, overnight at 4°C. After blocking the wells with 1% BSA in PBS for 1h at 37°C, wells were incubated with 5µg/mL of antibodies and controls diluted in PBS for 1h at room temperature. Increasing amounts of NHS diluted in GVB²⁺ were added and incubated for 45min at 37°C. Deposited C1q was then detected as described previously.

Animal procedures

The protocols were approved and performed in accordance with outlines in a license granted under the Animals (Scientific Procedures) Act 1986 and approved by the University of Liverpool Animal Ethics Committee (United Kingdom) or by the north ethical committee in Stockholm (Sweden). Eight week old male C57BL/6J or CD-1 mice (20-25g) were purchased from Charles River laboratories and had a 7-day acclimatization period in a 12h light/dark cycle and food and water was given *ad libitum* prior to experiments.

Mice (n = 6 or 10 for C57BL/6 or n = 7 for CD-1 mice) were fasted overnight for 15-16h. SI Figure1. Animals were challenged with an intraperitoneal (IP) injection of APAP (530mg/kg or 300mg/kg when indicated) or vehicle (0.9% saline). At 2h post-APAP (or 6h when indicated), mice were given 300µg of indicated antibody (or as

1
2
3 stated), 500mg/kg NAC or an equal volume PBS. At 10h post-APAP (or 24h when
4 indicated), mice were sacrificed using CO₂ and blood was taken by cardiac puncture.
5
6 Serum was isolated by centrifugation at 1500g for 10min at 4°C. Livers were snap
7
8 frozen in liquid nitrogen and stored at -80°C, or fixed in 4% PFA overnight at 4°C.
9
10

11 12 **Histological determination of hepatotoxicity**

13
14 Fixed liver sections were embedded in paraffin wax and 3µm sections were prepared
15
16 and stained with hematoxylin and eosin (H&E) or Periodic Acid Schiff (PAS) stain.
17
18 All sections were examined and the degree of hepatotoxicity was scored according
19
20 previously used criteria [3]. All examination and scoring of sections was performed
21
22 by Prof. A. Kipar, in a blinded manner.
23
24

25 26 **Immuno-histochemistry stainings**

27
28 Liver sections were deparaffinized in xylene and rehydrated with ethanol.
29
30 Subsequently, for antigen retrieval the slides were thermally processed in citrate
31
32 buffer (pH 6.0) using Retriever2100 (Electron Microscopy Sciences, Hatfield, PA,
33
34 USA) prior to immunostaining. To block endogenous peroxidase activity, sections
35
36 were treated with 1% H₂O₂ followed by a blocking buffer provided by the Histostain
37
38 kit (Life Technologies) followed by an avidin, biotin blocking step (Vector
39
40 Laboratories Inc., Burlingame, USA). The slides were thereafter incubated over night
41
42 with a rabbit anti-HMGB1 antibody (5µg/ml, ab18256, Abcam, Cambridge, MA,
43
44 USA) or rabbit anti-Ki67 antibody (abcam ab16667, diluted 1/100). For HMGB1,
45
46 immunochemical reactions were developed using the Histostain Plus 3-amino-9-
47
48 ethylcarbazol (AEC) detection system (Life Technologies) and Ki67 was visualized
49
50 using Bright Vision Ultimate DAB system (Immunologic, Duiven, Netherlands)
51
52 before counterstained with hematoxylin. In each assay, a primary rabbit
53
54 immunoglobulin of irrelevant antigen-specificity was included as a negative control
55
56
57
58
59
60

(Negative rabbit control, DAKO). Assessment of proliferation in the liver was performed by counting the number of Ki67 positive cells per mm² using Leica QWin V3 tips cell count image analysis program. In total, 7 fields per liver section were analyzed in 6 individual mice for m2G7, h2G7 and PBS. For E2 n=5.

Determination of total hepatic glutathione (GSH)

Total hepatic GSH was determined as described previously [4]. Briefly, 30-50mg of liver was homogenized in 800μL of GSH stock buffer (143mM NaH₂PO₄, 6.3mM EDTA, pH 7.4) supplemented with 200μL of 6.5% (w/v) SSA and incubated on ice for 10min in order to deproteinize samples. Homogenates were centrifuged (18400g, 5min, 4°C) and the supernatants stored at -80°C. The protein pellets were dissolved in 1M NaOH at 60°C for 1h and protein concentration of the dissolved pellet was determined using Bio-Rad protein assay (Bio-Rad Laboratories, Hemel Hempstead, UK). GSH content of the supernatants was measured by kinetic reaction (at 412nm) as previously described [5]. GSH in samples was compared to a 0 – 40 nmoles/mL standard curve and all samples were normalized to protein content.

Determination of alanine aminotransferase (ALT) activity in serum

Serum ALT activity was determined by kinetic assay according to the manufacturer's instructions (Thermo Scientific). 30μL of serum was loaded in duplicate into 96-well plates. ALT reagent was heated to 37°C and 300μL per well was added to samples and assayed at 340nm.

MicroRNA 122 (miR-122) quantification in serum

miR-122 was quantified in serum as previously described [6]. Total miRNA was extracted and purified using a miRNeasy kit followed by an RNeasy MinElute Cleanup Kit (Qiagen, Venlo, Netherlands), in accordance with the manufacturer's

instructions. The RNA was eluted in 14 μ L of nuclease-free water before storing at -80°C until further use.

Reverse transcription was performed using a TaqMan miRNA reverse transcription kit (Applied Biosystems) and miR-122 and Let-7d (endogenous miRNA control) primers. Briefly, 2 μ L purified miRNA was used to synthesise cDNA with a total reaction volume of 15 μ L via thermal cycling (30min at 16°C, 30min at 42°C, 5min at 85°C and then held at 4°C). Quantitative-PCR (qPCR) reactions were run in duplicate in 384-well plates using TaqMan PCR Primers and Master Mix (Applied Biosystems) according to manufacturer's instructions. 1.33 μ L of cDNA was used and the total reaction volume was made up to 20 μ L with primer/master mix, and subject to thermal cycling (2min at 50°C, 10min at 95°C and 50 cycles of 15sec at 95°C and 60sec at 60°C). miR-122 levels were subsequently normalized to the level of let-7d.

Chemo- and cytokine quantification in serum

Serum MCP-1, CXCL-1, TNF, IFN γ , IL-1 β and IL-6 concentration was determined by cytokine bead array (CBA) according to the manufacturer's instructions (BD Biosciences).

Statistical analysis

For *in vivo* studies, Kruskal-Wallis with Dunns post-test was performed. For *in vitro* data, two-tailed *t*-test was performed where indicated. All statistical analysis was performed using Graphpad Prism.

1
2
3
4
5
6
7
8
9
10
11
12
13
14
15
16
17
18
19
20
21
22
23
24
25
26
27
28
29
30
31
32
33
34
35
36
37
38
39
40
41
42
43
44
45
46
47
48
49
50
51
52
53
54
55
56
57
58
59
60

Supplementary Table 1.

Beneficial effects of m2G7 treatment in diverse experimental models

Year	Author	Effects of m2G7 treatment	Associated disease	
2005	Tsung A, <i>et al.</i> [7]	Reduced liver injury and inflammation	Ischemia / Reperfusion injury	Sterile inflammation
2010	Gao Q, <i>et al.</i> [8]	Reduced inflammation and improved pancreatic islet viability	Organ transplantation	
2011	Schierbeck H, <i>et al.</i> [9]	Reduced clinical signs of arthritis	Arthritis	
2014	Agalave NM, <i>et al.</i> [10]	Reduced pain hypersensitivity	Arthritis	
2014	Parker KH, <i>et al.</i> [11]	Reduced number of myeloid-derived suppressor cells in tumors	Cancer	
2015	Yang H, <i>et al.</i> [12]	Improved survival, reduced liver injury and inflammation	Acetaminophen-induced liver injury	
2006	Qin S, <i>et al.</i> [13]	Improved survival	Sepsis	Infectious
2012	Entezari M, <i>et al.</i> [14]	Protected against neutrophil recruitment, lung injury and bacterial infection	Pulmonary infection with <i>P.aeruginosa</i>	
2012	Chavan SS, <i>et al.</i> [15]	Reduced cognitive impairment	Sepsis	
2013	Achouiti A, <i>et al.</i> [16]	Reduced lung pathology and inflammation	Pneumonia	
2013	Patel VS, <i>et al.</i> [17]	Reduced bacterial counts and lung injury	Respiratory distress/ hypoxia	
2013	Valdés-Ferrer SI, <i>et al.</i> [18]	Reduced splenomegaly and inflammation	Sepsis	

Supplementary Table 2.

Cloning primes

use		sequence (5' – 3')	restriction site
IgG γ	forward	CTGCAACCGGTGTACATTCCCAGGTGCAGCTGCAGCAGTCTGG	AgeI
	reverse	TGCGAAGTCGACGCTGCAGAGACAGTGACCAGAG	Sall
IgG κ	forward	CTGCAACCGGTGTACATTCCGAAAATGTTCTCACCCAGTCTCCA	AgeI
	reverse	GCCACCGTACGTTTTATTCCAGCTTGGTC	BsiWI
HMGB1-HIS	forward	GCGCCATGGGCAAAGGAGATCCTAAGA	NcoI
	reverse	GCGCTCGAGTTCATCATCATCTTCT	XhoI
box A-HIS	forward	GCGCCATGGGCAAAGGAGATCCTAAGA	NcoI
	reverse	GCGCTCGAGGAACTCTTTTTGTCTCC	XhoI
box B-HIS	forward	AAGCCATGGGCAAAGGATCCCAATGCAC	NcoI
	reverse	GCGCTCGAGGACAACCTCTTTTGCT	XhoI
K322A	forward	CAAGGAGTACAAGTGC GCGGTCTCCAACAAAGC	
	reverse	GCTTTGTGGAGACCGCGCACTGTACTCCTG	

1
2
3
4
5
6
7
8
9
10
11
12
13
14
15
16
17
18
19
20
21
22
23
24
25
26
27
28
29
30
31
32
33
34
35
36
37
38
39
40
41
42
43
44
45
46
47
48
49
50
51
52
53
54
55
56
57
58
59
60

Supplementary Fig. 1

Schematic *in vivo* experimental overview. Mice were fasted for 15-16h before challenge IP with APAP (530mg/kg). At 2h post-APAP mice were treated with either PBS (vehicle) or 300µg of indicated antibodies. Mice were euthanized at 10h post-APAP. Serum ALT and miR-122 were measured as markers of hepatotoxicity and serum TNF, CXCL-1 and MCP-1 were used as markers of inflammation. Livers were harvested for histological analysis and to determine hepatic glutathione (GSH).

For Peer Review

Supplementary Fig. 2.

Antibody treatments alone do not affect the baseline levels of hepatic injury in non-APAP challenged mice. (A) Serum ALT or (B) serum miR-122 in non-APAP challenged C57BL/6 mice. Results are represented as means \pm SEM.

For Peer Review

1
2
3
4
5
6
7
8
9
10
11
12
13
14
15
16
17
18
19
20
21
22
23
24
25
26
27
28
29
30
31
32
33
34
35
36
37
38
39
40
41
42
43
44
45
46
47
48
49
50
51
52
53
54
55
56
57
58
59
60

Supplementary Fig. 3.

Representative liver from normal C57BL/6 mice stained with hematoxylin and eosin (H&E, upper left) or for HMGB1 expression (upper right). C57BL/6 mice exposed with APAP (530mg/kg) for 10h were stained were stained with either H&E (lower left) or for HMGB1 expression (lower right).

For Peer Review

Supplementary Fig. 4.

2G7 treatment reduces hepatocyte proliferation in APAP-challenged mice. C57BL/6 mice were challenged with APAP (530mg/kg) for 10h. At 2h post-APAP, mice were treated with either PBS (vehicle) or 300µg of indicated antibodies. The effect on hepatocyte proliferation was evaluated by Ki67 staining (n=6 for PBS, m2G7 and h2G7 and n=5 for E2 treated mice).

For Peer Review

1
2
3
4
5
6
7
8
9
10
11
12
13
14
15
16
17
18
19
20
21
22
23
24
25
26
27
28
29
30
31
32
33
34
35
36
37
38
39
40
41
42
43
44
45
46
47
48
49
50
51
52
53
54
55
56
57
58
59
60

Supplementary Fig. 5.

2G7 or box A does not affect APAP metabolism or liver injury markers in non-APAP exposed CD-1 mice. (A) Effect on hepatic glutathione (GSH) and GSH depletion following APAP exposure. (B) Treatments did not affect serum ALT in non-APAP challenged CD-1 mice. Results are represented as means±SEM

For Peer Review

Supplementary Fig. 6.

Effects of endoS treatment of h2G7. EndoS treatment of h2G7 dose-dependently affects its binding to (A) LCA, (B) human CD64 and (C) live THP-1 cells.

For Peer Review

1
2
3
4
5
6
7
8
9
10
11
12
13
14
15
16
17
18
19
20
21
22
23
24
25
26
27
28
29
30
31
32
33
34
35
36
37
38
39
40
41
42
43
44
45
46
47
48
49
50
51
52
53
54
55
56
57
58
59
60

Supplementary Fig. 7.

Effector function deficient h2G7 variants do not affect liver injury in APAP exposed mice. (A) Effect on serum miR-122 expression in C57BL/6 mice. Results are represented as means±SEM.

For Peer Review

Supplementary references

- [1] Tiller T, Meffre E, Yurasov S, Tsuiji M, Nussenzweig MC, Wardemann H. Efficient generation of monoclonal antibodies from single human B cells by single cell RT-PCR and expression vector cloning. *J Immunol Methods* 2008;329:112-124.
- [2] Amara K, Steen J, Murray F, Morbach H, Fernandez-Rodriguez BM, Joshua V, et al. Monoclonal IgG antibodies generated from joint-derived B cells of RA patients have a strong bias toward citrullinated autoantigen recognition. *J Exp Med* 2013;210:445-455.
- [3] Antoine DJ, Williams DP, Kipar A, Jenkins RE, Regan SL, Sathish JG, et al. High-mobility group box-1 protein and keratin-18, circulating serum proteins informative of acetaminophen-induced necrosis and apoptosis in vivo. *Toxicol Sci* 2009;112:521-531.
- [4] Williams DP, Antoine DJ, Butler PJ, Jones R, Randle L, Payne A, et al. The metabolism and toxicity of furosemide in the Wistar rat and CD-1 mouse: a chemical and biochemical definition of the toxicophore. *J Pharmacol Exp Ther* 2007;322:1208-1220.
- [5] Vandeputte C, Guizon I, Genestie-Denis I, Vannier B, Lorenzon G. A microtiter plate assay for total glutathione and glutathione disulfide contents in cultured/isolated cells: performance study of a new miniaturized protocol. *Cell Biol Toxicol* 1994;10:415-421.
- [6] Antoine DJ, Dear JW, Lewis PS, Platt V, Coyle J, Masson M, et al. Mechanistic biomarkers provide early and sensitive detection of acetaminophen-induced acute liver injury at first presentation to hospital. *Hepatology* 2013;58:777-787.
- [7] Tsung A, Sahai R, Tanaka H, Nakao A, Fink MP, Lotze MT, et al. The nuclear factor HMGB1 mediates hepatic injury after murine liver ischemia-reperfusion. *J Exp Med* 2005;201:1135-1143.
- [8] Gao Q, Ma LL, Gao X, Yan W, Williams P, Yin DP. TLR4 mediates early graft failure after intraportal islet transplantation. *Am J Transplant* 2010;10:1588-1596.
- [9] Schierbeck H, Lundback P, Palmblad K, Klevenvall L, Erlandsson-Harris H, Andersson U, et al. Monoclonal anti-HMGB1 (high mobility group box chromosomal protein 1) antibody protection in two experimental arthritis models. *Mol Med* 2011;17:1039-1044.
- [10] Agalave NM, Larsson M, Abdelmoaty S, Su J, Baharpoor A, Lundback P, et al. Spinal HMGB1 induces TLR4-mediated long-lasting hypersensitivity and glial activation and regulates pain-like behavior in experimental arthritis. *Pain* 2014;155:1802-1813.
- [11] Parker KH, Sinha P, Horn LA, Clements VK, Yang H, Li J, et al. HMGB1 enhances immune suppression by facilitating the differentiation and suppressive activity of myeloid-derived suppressor cells. *Cancer Res* 2014;74:5723-5733.
- [12] Yang H, Wang H, Ju Z, Ragab AA, Lundback P, Long W, et al. MD-2 is required for disulfide HMGB1-dependent TLR4 signaling. *J Exp Med* 2015;212:5-14.
- [13] Qin S, Wang H, Yuan R, Li H, Ochani M, Ochani K, et al. Role of HMGB1 in apoptosis-mediated sepsis lethality. *J Exp Med* 2006;203:1637-1642.

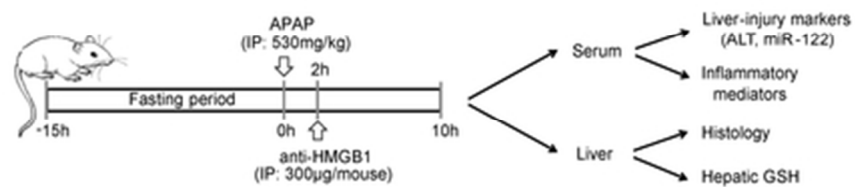
[14] Entezari M, Weiss DJ, Sitapara R, Whittaker L, Wargo MJ, Li J, et al. Inhibition of high-mobility group box 1 protein (HMGB1) enhances bacterial clearance and protects against *Pseudomonas Aeruginosa* pneumonia in cystic fibrosis. *Mol Med* 2012;18:477-485.

[15] Chavan SS, Huerta PT, Robbiati S, Valdes-Ferrer SI, Ochani M, Dancho M, et al. HMGB1 mediates cognitive impairment in sepsis survivors. *Mol Med* 2012;18:930-937.

[16] Achouiti A, van der Meer AJ, Florquin S, Yang H, Tracey KJ, van 't Veer C, et al. High-mobility group box 1 and the receptor for advanced glycation end products contribute to lung injury during *Staphylococcus aureus* pneumonia. *Crit Care* 2013;17:R296.

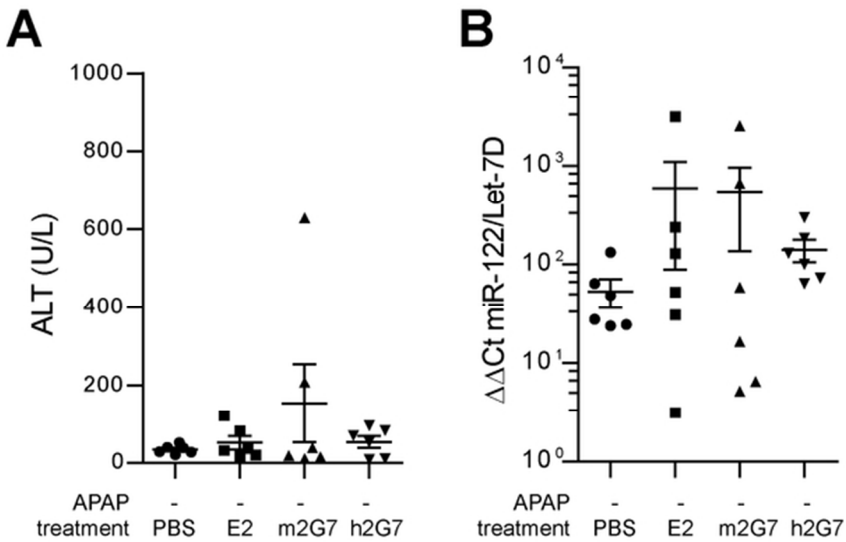
[17] Patel VS, Sitapara RA, Gore A, Phan B, Sharma L, Sampat V, et al. High Mobility Group Box-1 mediates hyperoxia-induced impairment of *Pseudomonas aeruginosa* clearance and inflammatory lung injury in mice. *Am J Respir Cell Mol Biol* 2013;48:280-287.

[18] Valdes-Ferrer SI, Rosas-Ballina M, Olofsson PS, Lu B, Dancho ME, Ochani M, et al. HMGB1 mediates splenomegaly and expansion of splenic CD11b+ Ly-6C(high) inflammatory monocytes in murine sepsis survivors. *J Intern Med* 2013;274:381-390.

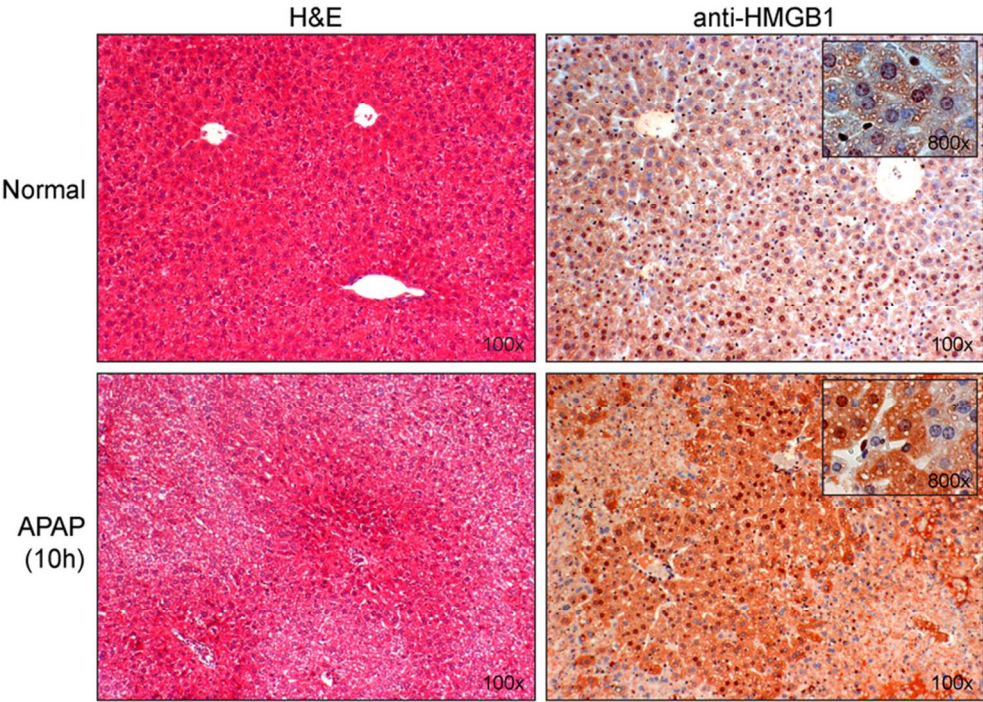


Supplementary Figure 1
37x10mm (300 x 300 DPI)

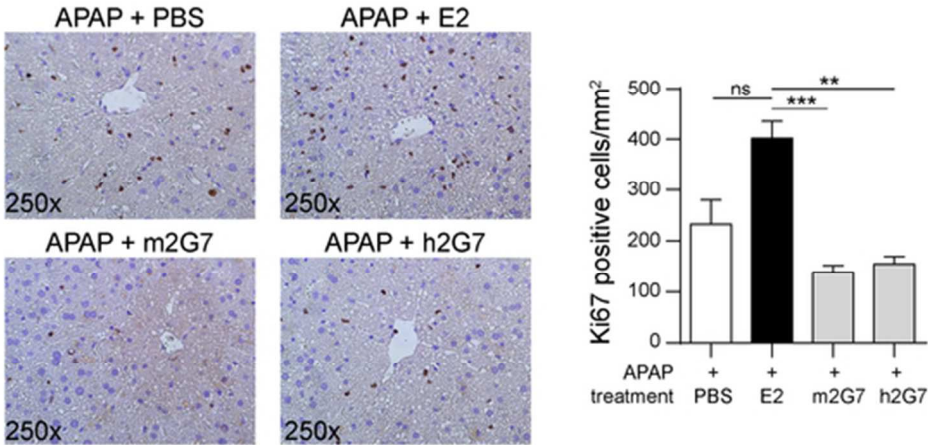
For Peer Review



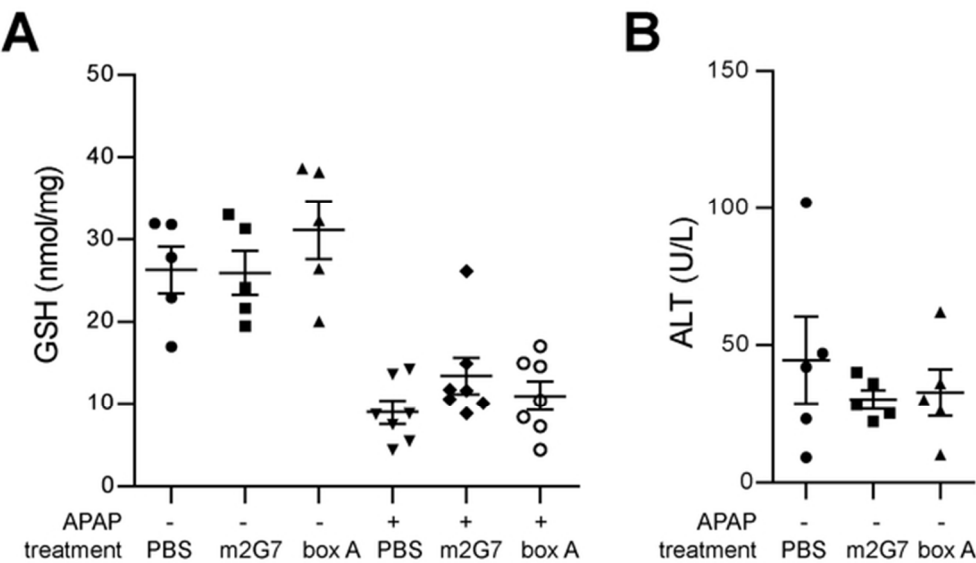
Supplementary Figure 2
60x38mm (300 x 300 DPI)



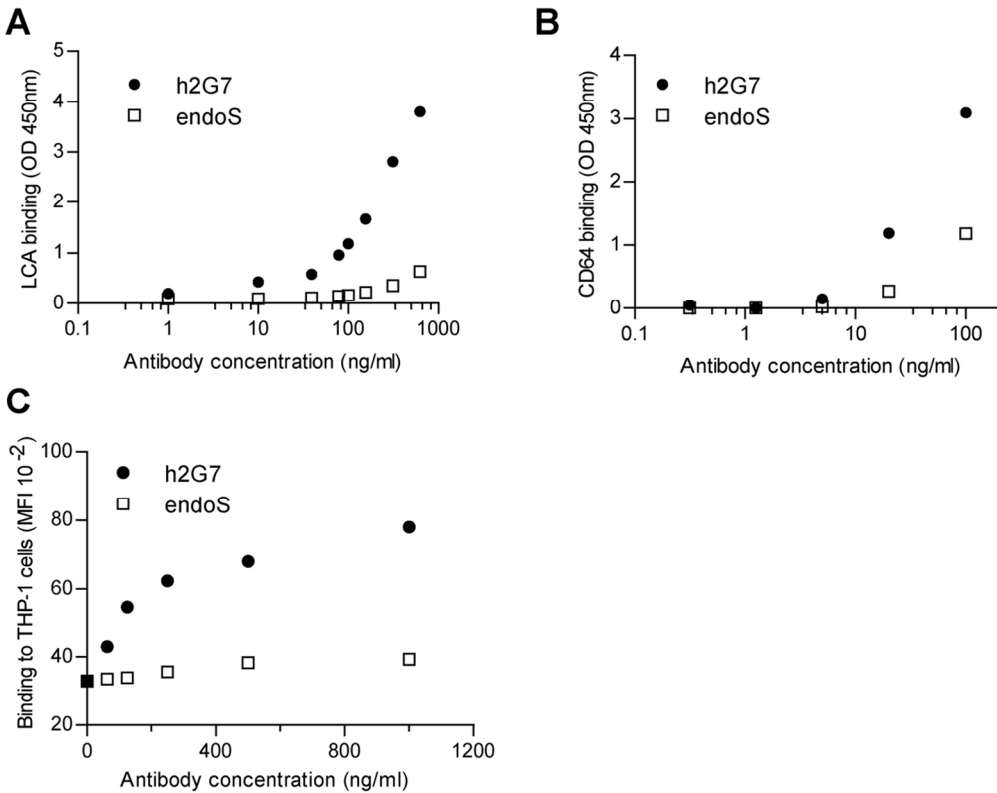
Supplementary Figure 3
76x54mm (300 x 300 DPI)



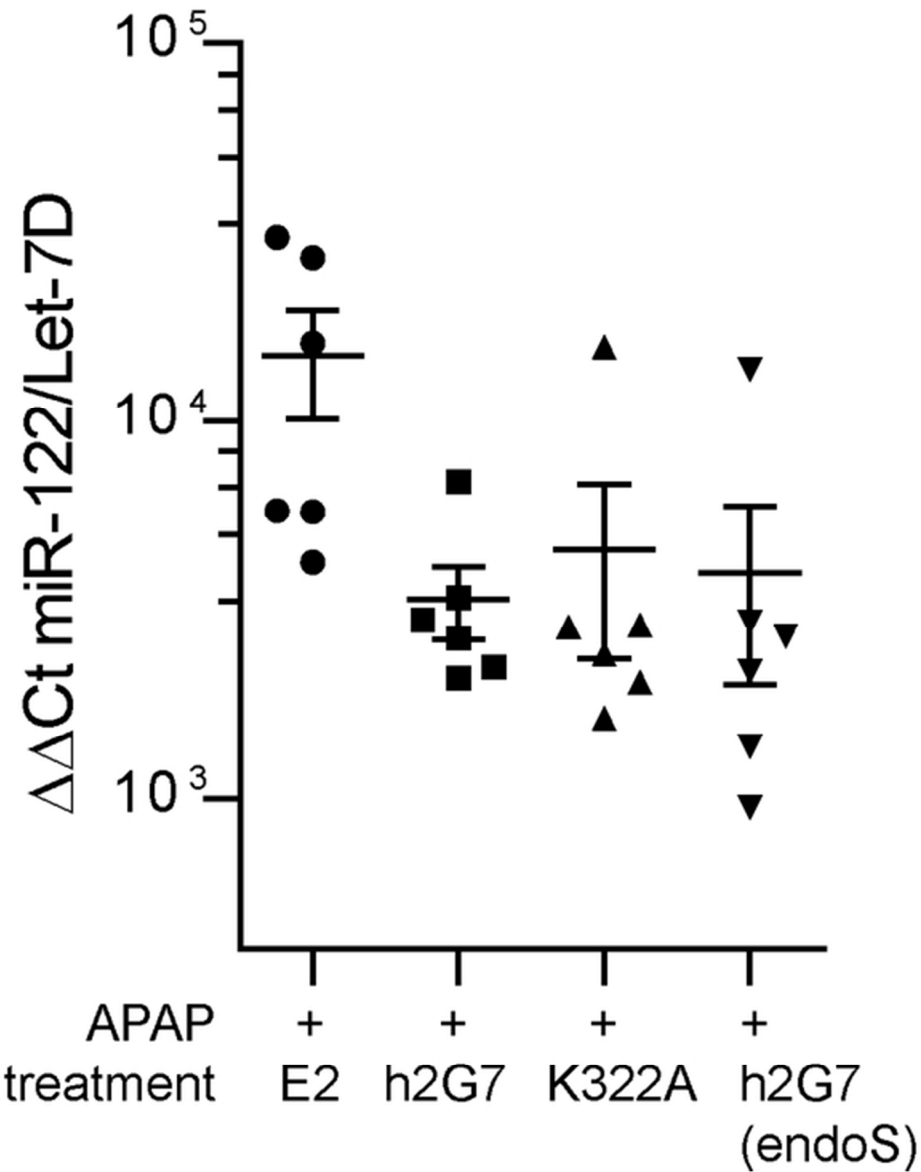
Supplementary Figure 4
49x22mm (300 x 300 DPI)



Supplementary Figure 5
55x34mm (300 x 300 DPI)



Supplementary Figure 6
109x87mm (300 x 300 DPI)



Supplementary Figure 7
50x63mm (300 x 300 DPI)